RIVAS

Railway Induced Vibration Abatement Solutions

Collaborative project

Measurement protocol for parameters influencing mitigation effects

Deliverable D1.2 Annex

Submission date:

03/08/2012

Project Coordinator:

Bernd Asmussen

International Union of Railways (UIC)

asmussen@uic.org

Title	**Measurement protocol for parameters influencing mitigation effects**
Domain	**WP 1.2**
Date	
Author/Authors	Adam Mirza, Alexander Smekal, Brice Nelain, David Thompson, Dorothée Stiebel, Geert Degrande, Geert Lombaert, Hans Verbraken, Rüdiger Garburg, Vicente Cuellar
Partner	DB, SBB, SNCF, Trafikverket, Vibratec, ISVR, BT, RATP, KUL, CSTB, Cedex , Adif, BAM
Document Code	rivas_db_wp1_d1_2_annex_v02_measuring_influencing_parameters
Version	4
Status	Final

Dissemination level:

Project co-funded by the European Commission within the Seventh Framework Programme		
Dissemination Level		
PU	Public	X
PP	Restricted to other programme participants (including the Commission Services)	
RE	Restricted to a group specified by the consortium (including the Commission) Services)	
CO	Confidential, only for members of the consortium (including the Commission Services)	

Document history		
Revision	Date	Description
1	18/05/12	First draft version
2	19/06/12	Second draft version
3	11/07/12	Third draft version
4	03/08/12	Final version

1. EXECUTIVE SUMMARY

The aim of the RIVAS project is to develop mitigation measures at source, track, propagation path and vehicle [1]. For the mitigation measures developed, the efficiency has to be obtained by measurements. In order to ensure the comparability of results measured by different partners, a common measurement procedure was elaborated which describes how the efficiency is measured and analysed [2]. Because the measuring conditions can be different compared to the reference conditions as defined in the RIVAS project, the mitigation-measure efficiency has to be recalculated for a reference situation including parameters for the excitation, the train, the track, and the soil. For this recalculation, a model based on a transfer function coupling the excitation to the vibrations response will be used. Therefore also measuring protocols for parameters influencing mitigation-measure efficiencies are needed. This is part of the deliverable D 1.2 Annex which is an additional document not announced in the list of RIVAS deliverables.

In section 3.1, a simplified modelling approach based on the rail unevenness U_R, the wheel unevenness U_W, the track receptance A_R, the vehicle receptance A_W, and the transfer function H is presented. For the measurement, there are two possibilities to characterize the measuring and the reference conditions. First, the influencing parameters U_R, U_W, A_R, A_W and H can be measured directly. The second possibility includes calculation of U_R, U_W, A_R, A_W and H based on measurements of the basic parameters (e. g. by knowing the masses and the elastic properties of the vehicle suspension, the vehicle receptance A_W can be calculated by using simple models). Both approaches will be considered in this report.

In section 3.2, methods to determine wheel and rail unevenness (U_R, U_W) as well as the stiffness variation along the track are described. Section 3.3 summarizes the measurement protocol to determine dynamic soil characteristics and transfer functions H. For the track characterization, a measuring protocol for the track receptance A_R as well as for the stiffness and damping of resilient elements in the track can be found in section 3.4. As discussed in section 3.5, the vehicle receptance A_W is typically calculated by using the stiffness and damping of the primary suspension and the masses included.

The measuring protocols for the different influencing parameters differ in the degree of detail. Where ever possible, reference is made to standards and the description is kept brief. But if no standards are available, as for the soil characterization or the measurement of the wheel unevenness the measuring protocols are more detailed. Although the authors are aware that e. g. the measurement protocol for the ballast parameters is missing, it was decided to make the document accessible to the partners as soon as possible. If new results are obtained within the RIVAS project, the document can be updated if necessary.

2. TABLE OF CONTENTS

3. CHAPTERS

3.1 INTRODUCTION

The aim of the RIVAS project is to develop mitigation measures at source, track, propagation path and vehicle [1]. For the mitigation measures developed, the efficiency has to be obtained by measurements of the insertion loss. In order to ensure the comparability of results measured by different partners, a common measurement procedure was elaborated which describes how the efficiency is measured and analysed [2]. Because the measuring conditions can be different to the reference conditions as defined within the RIVAS project, the mitigation-measure efficiency has to be recalculated for a reference situation including parameters for the excitation, the train, the track, and the soil. For this recalculation, a model based on a transfer function coupling the excitation to the vibrations response will be used. This model will be described in the following subsections.

3.1.1 Theoretical basis

Ground borne noise and vibrations are caused by several types of excitation:

- The **quasi-static excitation**, related to the train load moving at a given speed. This will not propagate in the ground as long as the lowest wave speed in the ground is greater than the train speed.
- The main excitation is described as a **relative displacement** at the wheel and rail contact point. It is usually referred to as wheel and rail unevenness and can include isolated unevenness (such as wheel flats, welded joints…).
- The **parametric excitation** is related to the stiffness variation of the track. It generates high vibration levels at the sleeper passing frequency and its harmonics, but can also include lower frequency components, that can be described by random variation of the ballast stiffness for instance. Unlike the unevenness, the parametric excitation depends on the train static load (the higher the load, the higher the contact force) and also depends on the track stiffness (the lower the stiffness, the lower the excitation).

Assuming that the relative displacement excitation is the predominant source of excitation, the physical phenomena involved in the generation and propagation of ground vibration due to rolling stock pass-by can be expressed by two simplified equations in the frequency domain [3].

$$F_{contact} = \frac{U_R \oplus U_W}{A_R + A_W (+A_C)} \tag{1}$$

$$v_{ground} = H \cdot F_{contact} \tag{2}$$

The first equation relates the wheel / rail contact force ($F_{contact}$) to the incoherent sum of the wheel and rail unevenness ($U_R \oplus U_W = \sqrt{U_R^2 + U_W^2}$), using the track, vehicle and Hertzian contact receptance (A_R, A_W and A_C). The track receptance A_R depends on track, sub-grade and soil properties. The vehicle receptance A_W depends on vehicle properties. This equation represents the interaction between the track and the train.

The second equation relates the same contact force to the ground vibration level away from the track (v_{ground}), using a transfer function (H), which depends on soil and track characteristics.

The Hertzian contact receptance A_C is low compared to vehicle and track receptance and can be neglected in the equation. This equation represents the propagation of the vibration in the track and ground.

Hence (1) and (2) are combined in:

$$v_{ground} = \left(\frac{H}{A_R + A_W} \right) \cdot \left(U_R \oplus U_W \right) \qquad (3)$$

The last equation (3) shows that the ground response is completely described if all terms of the equation are known. The equations are given in the frequency domain: each parameter of the equation is a function of the frequency $f = V/\lambda$ defined as the ratio between the train speed V and the uneveness wavelength λ.

These equations are based on some reasonable assumptions such as:

- No influence of wheel/rail lateral dynamic force and cross-coupling on ground vibrations.
- Linear relationship between forces and vibration displacement.
- No coupling between the two rails through the axle.

Although parametric excitation is not included in this approach, effects arising e. g. by stiffness variations along the track or sleeper passing effects might be considered under some assumptions by using an effective rail unevenness.

Equation (3) is illustrated in Figure1.

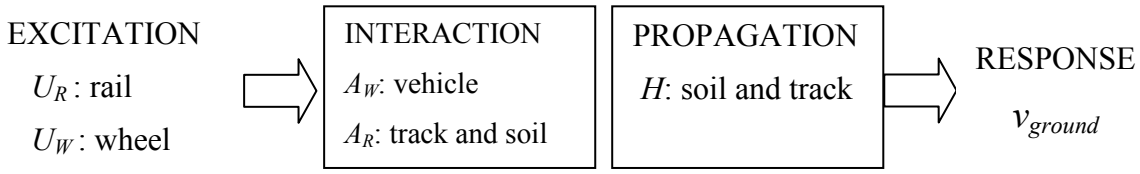

Figure 1: Illustration of equation (3)

Two options can be considered to reduce ground vibration:

- Reduce the excitation: If the system is linear (which is reasonably assumed here), then dividing the excitation by a given factor will divide the vibration by the same factor. In this case, there is no need for the transfer of the insertion loss. The reduction spectrum will be directly applied on the ground vibration spectrum.
- Modify the train, track or propagation path: In this case, the insertion loss recalculation requires a complete description of the measuring and the reference situation. Consequently, the following parameters should be characterized for a complete assessment of a given mitigation measure: vehicle receptance, track receptance, and transfer function.

In the next step, the measuring procedures for the mitigation-measure efficiency from deliverable D 1.2 [2] are analysed considering the parameters mentioned above:

- **Procedure 1** (Comparison of vibration levels obtained at adjacent sections with and without measure):

  For this procedure, the vehicle receptance (A_W) and the wheel unevenness (U_W) will not differ on the two sections (with and without mitigation) as the same trains pass by.

The track receptance (A_R) and the transfer function (H) can change due the variation of the soil from one site to another (even for sections just some hundred metres apart from each other).

The influence of the rail unevenness (U_R) between the two sections can be minimized by choosing trains for which the wheel roughness is predominant. On the same section, if the ground vibration levels show a discrepancy of more than 5 to 6 dB between two trains belonging to the same train category, then the wheel roughness is predominant compared the rail roughness.

- **Procedure 2** (Comparison of the vibration levels before and after the installation of a measure):

  The rail roughness can vary before and after the installation. To minimize the influence, the time interval between measurements before and after installation should be minimized. However, if the track is reconstructed as part of the installation then it cannot be assumed that its roughness is unaffected, especially at longer wavelengths.

  The influence of the wheel unevenness can be minimized by averaging on many pass-bys of trains within the same train category.

  The vehicle receptance will vary slightly within a given train category.

  The transfer function (depending on track and soil parameters) and the track receptance vary when installing mitigation measures at track or in the propagation path.

- **Combined procedure:**

  If the reference section is not modified between measurements, the influence of the wheel and rail unevenness is expected to be minimal.

  The vehicle receptance will vary slightly within the same train category. The track receptance and the transfer function will vary when installing mitigation measures at track or in the propagation path.

3.1.2 Recalculation procedure from measuring to reference conditions

For the transfer of the mitigation-measure efficiency from the measuring conditions to the reference conditions, the physical phenomena involved in ground-vibration generation and propagation have to be considered. The key of the transfer is to correctly characterize the phenomena by measurements and databases of dynamic properties of components, and simulations.

The transfer procedure is illustrated in Figure 2:

- Field measurement of the insertion loss under given measuring conditions (vehicle, track, soil, excitation)
- Characterization of the measuring conditions by the determination of vehicle, track, soil properties and the determination of the predominant type of excitation

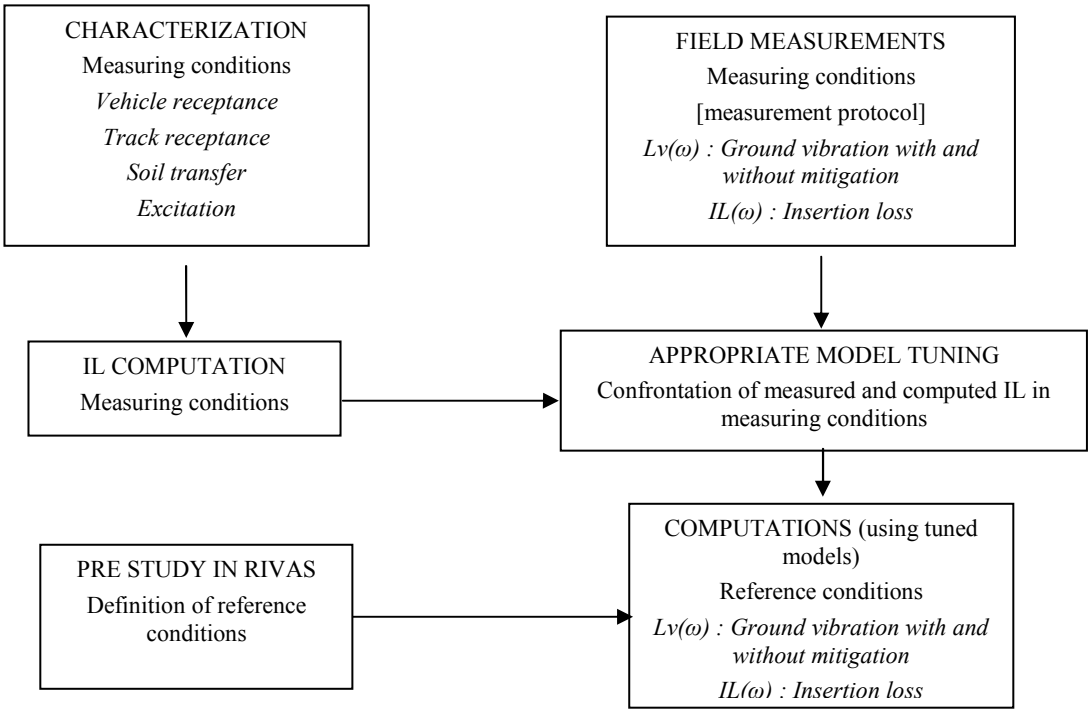

Figure 2: Transfer procedure flow chart (IL: insertion loss)

- Computation of the insertion loss in the situation the measurement had been performed (measuring situation), using previous characterization; comparison to the measured insertion loss: assessment of the robustness of the computation, model validation.
- Recalculation of the insertion loss for reference conditions by computation using the validated model.

3.1.3 Parameters influencing the mitigation-measure efficiency

For the characterization of the measuring and the reference configuration, two possibilities for characterization exist. First the rail unevenness (U_R), the wheel unevenness (U_W), the track receptance (A_R), the vehicle receptance (A_W) and the transfer function (H) can be measured directly. The second possibility includes calculations of U_R, U_W, A_R, A_W and H based on measurements of the basic parameters (e. g. by knowing the masses and the elastic properties of the vehicle suspension, the vehicle receptance A_W can be calculated by using simple models). Both approaches will be considered in this report.

3.2 EXCITATION CHARACTERIZATION

3.2.1 General aspects

As discussed in section 3.1, the excitation characterization is mainly of importance if procedures 1 or 2 of the measuring protocol are used for the detection of the insertion loss. The combined procedure tends to minimize the influence of the excitation. But the measurements of the excitation are important if models have to be tuned to absolute vibration measurements or if the roughness is not the predominant source of excitation.

In the following, methods to determine wheel and rail unevenness as well as stiffness variation along the track will be described. Here, wheel unevenness means the deviation of the wheel surface from a perfect round surface. Likewise, rail unevenness is the deviation of the real rail surface from a perfect flat surface. In a general approach, rail unevenness can also include effects due to stiffness variation of the track.

3.2.2 Wheel uneveness U_W

There is currently no national or international standard for the measurement or analysis of wheel roughness. Indeed, wheel roughness measurements are far less commonly carried out than those for rail roughness. The procedure for wheel roughness proposed here is based closely on EN 15610:2009 [4]. Reference has also been made to the measurement specification for wheel roughness recommended from the NOEMIE project [5].

As in EN 15610:2009 [4], methods for selecting measuring positions, data acquisition, data processing to estimate a set of one-third octave band spectra and the presentation of the results are proposed.

The purpose of such a measurement is to quantify the wheel roughness of a vehicle or a train for comparison with the rail uneveness, for comparison with various reference spectra or for use in prediction models.

Measuring system requirements

Testing and approval of measurement apparatus are not part of the scope of the present procedure. The requirements of the measurement system are defined solely in terms of output data and parameters relevant to the output data.

The following arrangement is envisaged (although other possible arrangements may be allowable):

- The wheel set will be jacked clear of the rail by a distance sufficient to allow free rotation.
- One or more probes will be located against the running surface using the rail as a reference.
- The wheel will be rotated either by hand or by a dedicated motor arrangement.

Accuracy: The measuring system shall be capable of making valid measurements in the wavelength range and at the relevant roughness levels for the wheel being characterized. For the purposes of the RIVAS project this means that at least wavelengths in the range 40 to 400 mm shall be measured. In addition the various harmonics of the out-of-roundness must be measured for wavelengths longer than this.

Dimension of the probe: If a contact probe is used, the probe tip shall be spherical and its radius shall not exceed 7 mm. For a non-contacting sensor, its effective width shall be less than the sampling distance.

Sampling interval: The measuring system shall provide data with a fixed and known spatial sampling interval less than or equal to 1 mm.

Record length: The system shall be capable of measuring record lengths of at least one complete circumference of the wheel at a time.

Selection of wheels

If it is not possible to measure all wheels of a train, measurements shall be made of a representative number of wheels:

1. For measurements of a single vehicle, at least 4 wheels shall be measured, distributed on both sides of the vehicle (they may include wheels at both ends of the same axle);
2. For a whole train, at least 10 wheels, distributed on both sides of the train (or one quarter of all wheels if this is greater);
3. Where both powered and unpowered wheels are present in a train, the measured wheels should include at least 4 powered and 4 unpowered wheels (or at least one quarter of each category of wheel if this is greater than 4);
4. Where different wheels in a train have different braking systems, at least 4 wheels of each type of braking system should be included (or at least one quarter of each category of wheel if this is greater than 4).

For each category of wheel identified in points 3 and 4, the samples should be distributed over the whole train and on both sides. The report should indicate clearly which wheels have been measured.

Wheel Uneveness

Unless it is the purpose of the measurements to quantify them, specific wheel uneveness such as wheel flats should be omitted from the measurement. If possible this should be done by avoiding wheels containing such uneveness; otherwise they should be removed from the data (see Data processing below).

If necessary the wheels should be cleaned before making the measurements in order to remove surface contamination.

Measurement zone

It is the responsibility of the measurement team to define the lateral position and width of the reference surface on the wheel and to justify its decision.

Where a clear running band is visible on the wheel tread, the measurement zone shall be located in this visible band. At least three lines of measurement shall be made 10 mm apart across the wheel tread. If relevant, positions at 60, 70 and 80 mm from the flange-back shall be used out of preference for a standard main line tyre width of 135 mm (provided that they are within the running band). Additional lateral positions between or beyond these positions may also be used in order to

cover the running band. Where possible the measurements at all lateral positions should be synchronized relative to each other.

At each position at least two full circumferences of the wheel shall be measured.

Data processing

(a) The data shall be processed in three steps before calculating the wavelength spectrum:

1. Cut out data contaminated by wheel uneveness.
2. Process the data so as to remove narrow upward spikes that are regarded as being linked with the presence of small particles of foreign matter on the wheel surface ('spike removal' process).
3. Process the data to take account of the effect of the small radius of the probe tip compared with that of the wheel ('curvature processing').

Stages 2 and 3 shall always be carried out in this order. The removal of unevenness (stage 1) may be carried out either before or after stages 2. and 3.

EN 15610:2009 contains advice and example measurements of features that should, and should not be, regarded as uneveness on the rail head. Corresponding criteria should apply for the wheel roughness measurements.

Other effects such as the 'contact filter' are not within the scope of this procedure.

(b) Calculate the one-third octave band spectrum for each acoustic roughness record using the Fourier analysis method specified in EN 15610:2009 [4]. The 1/3 octave filtering method should not be used.

(c) Estimate the mean acoustic roughness spectrum for the vehicle or train using an energetic average. An indication of the statistical distribution should also be given.

For the above steps, identical processing shall be used as specified for the rail in EN 15610:2009 (not repeated here) except for the following differences [4].

I. In step (b) windows and multiple data segments shall not be used: the data segment shall have a length equal to one revolution of the wheel and shall be analysed using a single Discrete Fourier Transform without zero padding. The number of samples corresponding to the circumference of the wheel shall be determined by a suitable method. For example:

- Difference methods, where the estimated circumference is varied and the sum of squared differences is minimized over points one test circumference apart;
- Using an auto correlation method.
- Mechanically by the measurement device.

II. In step (c) allowance should be made for the number of powered and unpowered wheelsets and a weighted average used as appropriate. Similarly, if there are different braking mechanisms on different vehicles of the train, allowance should be made for the number of each within each noise measurement section of the train.

The repeatability of the measurement shall be checked by comparing the profile measurement records from successive rotations of the wheel.

Advisory note:

Attention should be paid to avoid the following sources of error.

- Movement of the wheel can occur due to the effort of turning it during the measurement.
- The tachometer tracking of the measurement may slip on the wheel tread during measurement.

Documentation

Similar to EN 15610:2009 [4], the data shall be presented in the form of:

(a) An acoustic roughness graph in one-third octave bands with the roughness level plotted as a function of wavelength, in decreasing order. This may be accompanied by a reference spectrum if necessary (not mandatory). The range of wavelengths shall contain at least one-third octave bands for the wavelengths between 400 mm and 40 mm. The numbering of the wavelength labels shall correspond to the preferred frequencies of EN ISO 266 [6].

If it is required for the subsequent use of the data, average spectra over the different wheels for each of the lateral positions on the tread shall be presented.

(b) A table of the associated one-third octave spectrum data.

(c) In addition, the peak amplitude of the first 10 out-of-round harmonics shall be tabulated. This shall be presented for central line of roughness only.

The wheel diameters shall also be determined and stated.

Plots of the circumferential profile data may also be included.

The test report shall contain the presentation of the results as specified in above. In addition the following shall be included:

(a) Description of the train including the position in the train of each wheel that has been measured and an indication of which are driven / trailer and the type of braking system for each wheelset.

(b) Distance or time since reprofiling where this is known.

(c) Wheel diameters (and state of wear).

(d) Precise lateral position of the measurement in terms of the distance of each measurement line to the flange-back.

(e) Manufacturer, type and serial number or other means of identification of the measuring equipment.

(f) Photographs of the wheel surface with an indication of the position of the reference surface and measurement lines.

3.2.3 Rail uneveness U_R

The wavelength range that is required depends on the frequency range and train speed. For frequencies of 4 to 250 Hz and train speeds from 40 to 200 km/h a wavelength range is required (rounding to the nearest standard one-third octave band) of

- 3 m to 40 mm at 40 km/h, and
- 16 m to 200 mm at 200 km/h.

So the overall wavelength range can be considered as 16 m to 40 mm.

For wavelengths greater than 1.2 m (twice the sleeper spacing) the geometry of the track support structure determines the unevenness, whereas for wavelengths shorter than 1.2 m the roughness of the rail itself is important and the foundation geometry has no effect. The sleeper passing effect at a wavelength of 0.6 m can also be important.

For the measurement of the unevenness, the effect of loading can have a strong influence. At the longer wavelengths (greater than 1.2 m) it is the loaded geometry that determines the effective unevenness U_R that is the input to the wheel/rail system. The sleeper passing effect is also dependent on the wheel load. Apart from the sleeper-passing effect, however, at wavelengths shorter than 1.2 m the loading is unlikely to have a significant effect and it is sufficient to measure the unloaded roughness.

Measurement of rail roughness by trolley systems

For shorter wavelengths the rail roughness can be measured using acoustic roughness devices. There are two main types of rail roughness device: fixed length beams such as the RM1200 or ODS systems and trolley systems such as the CAT trolley. A fixed length beam is limited to short wavelengths (usually one-third octave bands shorter than 100 mm) and although it is acceptable for acoustic measurements this is not sufficient for ground vibration. Therefore it is necessary for these measurements to use a trolley system.

Trolley systems such as the CAT use an inertial reference and rely on double-integration of the acceleration signal to obtain displacement. Consequently, although results can be obtained at long wavelengths, it is recommended to limit the results to a maximum wavelength of 2 m. To obtain this the parameters of the high pass filter have to be chosen appropriately. It has to be demonstrated that the long wavelengths are valid (for example by comparison with the output from the track recording car).

The measurement and analysis of rail roughness is described in the standard EN 15610:2009 [4] and this is not repeated here. The main difference for the present application is that the required wavelength range is 2 m to 40 mm.

Measurement of rail unevenness by track recording cars

Because measurement and analysis procedures of track recording cars used by the RIVAS partners are different, a common procedure is not possible. Therefore data from track recording cars should be used mainly to compare the rail unevenness at test sites e. g. with and without mitigation measure of the same measurement campaign.

Track recording cars usually produce derived data in terms of track geometry which is often filtered to exclude shorter wavelength components. For the present purpose it is necessary to obtain ‘raw’ unfiltered data sampled at as high a rate as possible, ideally to cover the full wavelength range 16 m to 40 mm.

But unevenness amplitudes decrease as the wavelength decreases, which means that short wavelength unevenness may not be resolved correctly by track recording cars. Moreover the measurement principle is not guaranteed to yield valid data at short wavelengths (frequencies above

about 80 Hz). Therefore it has to be shown whether the data produced is valid at short wavelengths. For this it is advisable to use also rail roughness measurement in parallel as shown in the following example.

Example

Two examples of measured data from a track recording car and a roughness trolley are shown in Figure 3 below [7]. In the first case the track recording car data was filtered at a wavelength of 1 m and in the other case (using a different system) at a wavelength of 3 m. Here, the data from the track recording car and the CAT trolley do not match perfectly due to the limitations of both methods but they can be seen to be generally consistent in the region where they overlap.

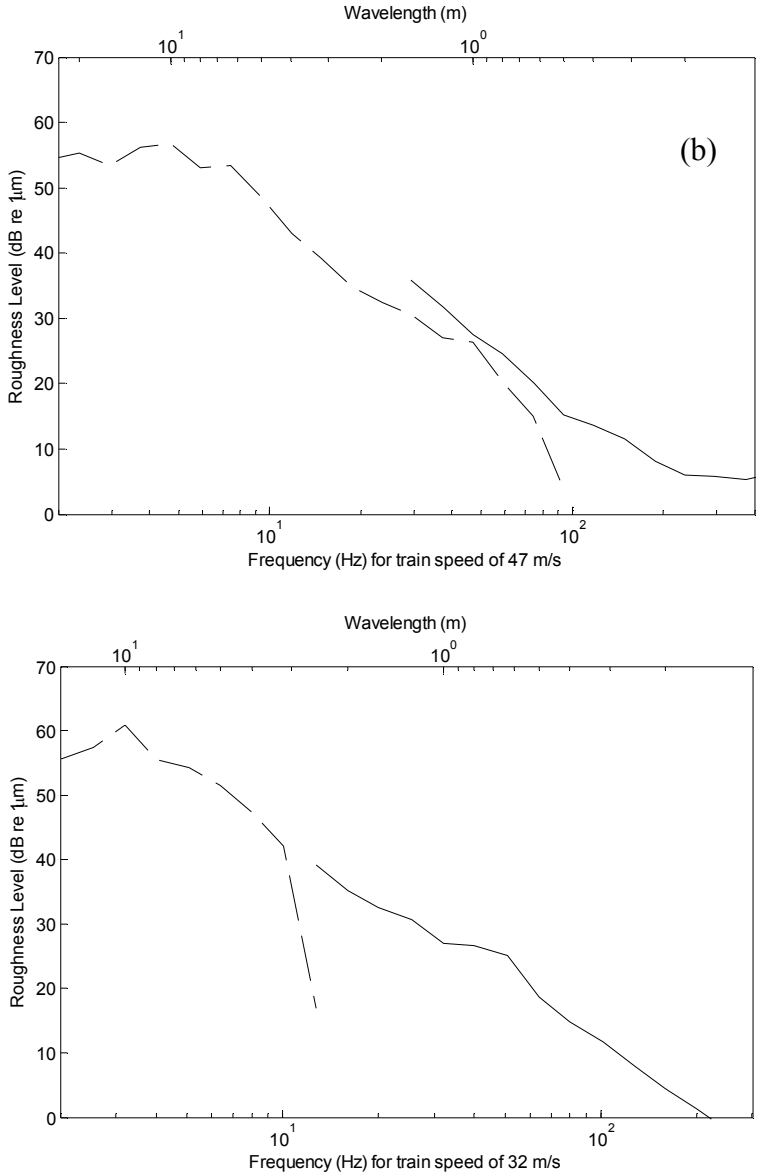

Figure 3: Roughness spectra in one-third octave bands obtained at two sites. —, measured using CAT trolley; – – –, measured using track recording coach. (a) Steventon, (b) Grazeley Green [7].

3.2.4 Track stiffness variation along the track (for calculating an effective U_R)

Track stiffness measurements are of great interest for maintenance monitoring, because the track stiffness is closely linked to track and substructure quality. The main measurement methods were described by Berggren in his PhD thesis [8]. This review is mainly based on his work.

The vertical track stiffness measurements methods can be classified in two categories: standstill measurements and rolling measurements. The standstill measurements are performed on a restrained part of the track and need traffic to be stopped. They are mainly used for research purposes. The rolling measurements have the advantages of covering long lengths of track.

Tables 1 and 2 summarize the main methods for both types of measurements (extracted from [8]).

STANDSTILL MEASUREMENTS.

Method	Frequency range	Preload	Advantages	Disadvantages
On track measurements: instrumentation of rail and pads with strain gauges, accelerometers and displacements transducers.	Quasi-static Load – deflection curve Dynamic [0 – 300 Hz]	Train pass-by	Simple setting on a portion of the track	Needs to record several adjacent sleepers to cover a wheel perimeter
Impact hammer	[50 – 1500 Hz]	Standstill train / preload	Simple	Need train preload
Falling weight deflectometer (FWD)	Depends on the impact	125 kN (UK)	Lots of configurations can be tested	Time-consuming
Track loading vehicle (TLV)	Up to 200 Hz	150 kN (Sweden)	Lots of configurations can be tested Track lateral stability	Time-consuming

Table 1: Overview of standstill measurements – advantages and disadvantages

ROLLING MEASUREMENTS.

Method	Frequency range	Advantages	Disadvantages
Differential load on coaches 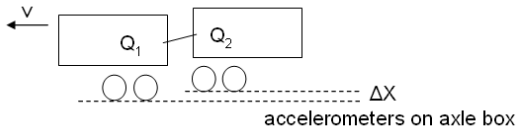 (e.g.: CARS – China , TTCI – USA, SBB - Switzerland	[0-50 Hz]		Access to static stiffness only
Rolling stiffness measurement vehicle (RSMV, used in Eurobalt and Innotrack) 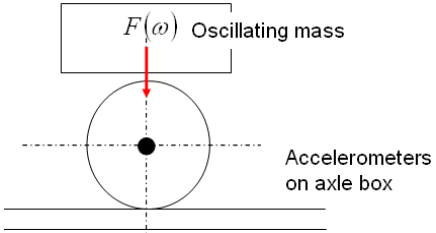	[0-50 Hz]	Validated in European projects Access to quasi-static and dynamic stiffness	Need dedicated vehicle Costly

Table 2: Overview of rolling car measurements

Track stiffness measurements in RIVAS project have two objectives:

- Provide local track stiffness for tuning purpose: this requires standstill measurements,
- Provide the parametric excitation (stiffness variation): this requires continuous measurements over a consequent length of track.

Measurement of the track stiffness by standstill methods using regular trains

The chosen protocol has the advantage of being performed during train pass-by and can hence be directly combined to ground vibration measurements foreseen in the frame of the RIVAS project.

Description of the instrumentation:

For several train pass-bys, recordings will be performed on several adjacent sleepers (see Figure 4) to cover a complete wheel perimeter (15 sleepers will cover 8.4 metres corresponding to about 3 wheel perimeters):

- Relative displacement of the rail pads: ΔX (difference of displacement between rail and sleepers). The rail-pads are used as a force transducer by preliminary characterisation of their static and dynamic stiffness in the laboratory. The force F=K.ΔX transmitted through the rail-pads is then known.
- Sleeper acceleration. A double integration will give the sleeper deflection: Ds.

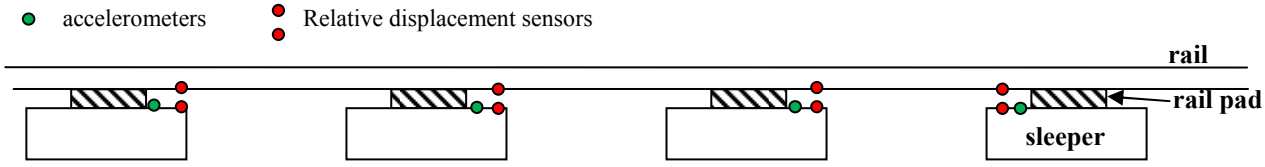

Figure 4: Measurement of relative displacements and sleeper deflexion

This measurement can be completed by a direct force measurement using strain gauges on the rail (Figure 5).

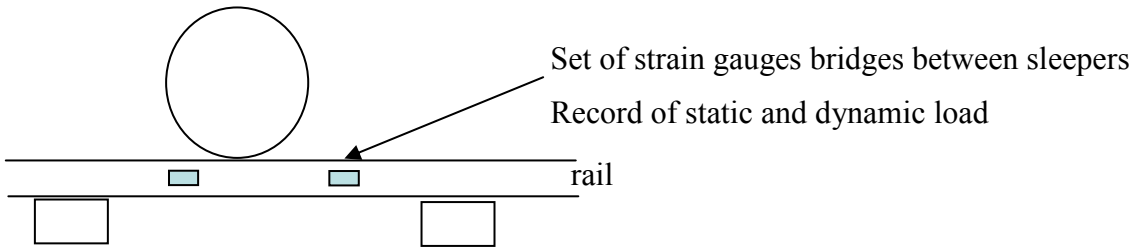

Figure 5: Measurement of contact force using strain gauges on rail

Number of measurement channels:

Ideally, 15 adjacent sleepers should be instrumented:

- 30 relative displacement sensors (15 on each rail)

- 30 acceleration sensors (15 below each rail)

If it is not possible, the minimum requirements are:

- 22 relative displacements (11 on each rail)
- 14 acceleration sensors (7 below each rail)

Determination of track stiffness:

The stiffness seen from the sleeper is determined by $K_{sleeper}$ = F/Ds. Then the track stiffness can be derived by simple calculation or simple modelling.

The measured stiffness seen from the sleeper will be presented as a graph of force versus displacement as presented in Figure 6. This method can also highlight hanging sleepers (Figure 7). The results are averaged on all measured sleepers.

The measurements must be performed at a low speed train (~ 20 kph) to obtain the quasi-static value, and can be performed with higher speed to determine dynamic values.

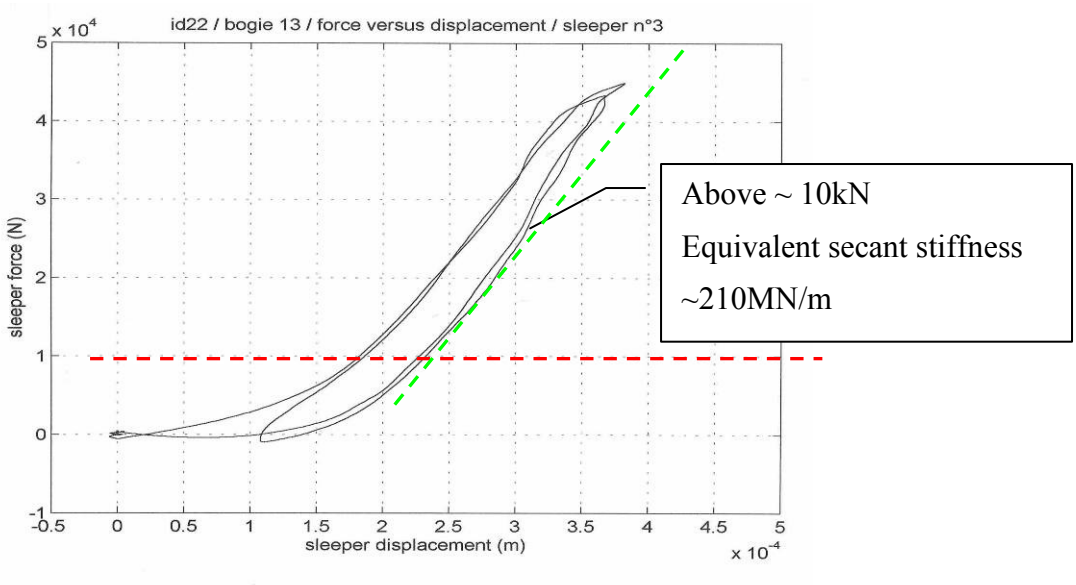

Figure 6: Measurement of relative displacements and sleeper deflexion

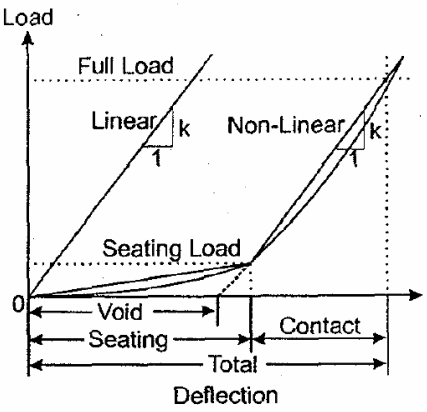

Figure 7: Illustration of voids and non-linearities [8]

Determination of static and dynamic contact force:

The contact force versus time is calculated by the summation of the adjacent force signals F versus time, as illustrated in Figure 8. This process should be valid below about 100 Hz, at which frequency the inertia effects of the rail can no longer be neglected.

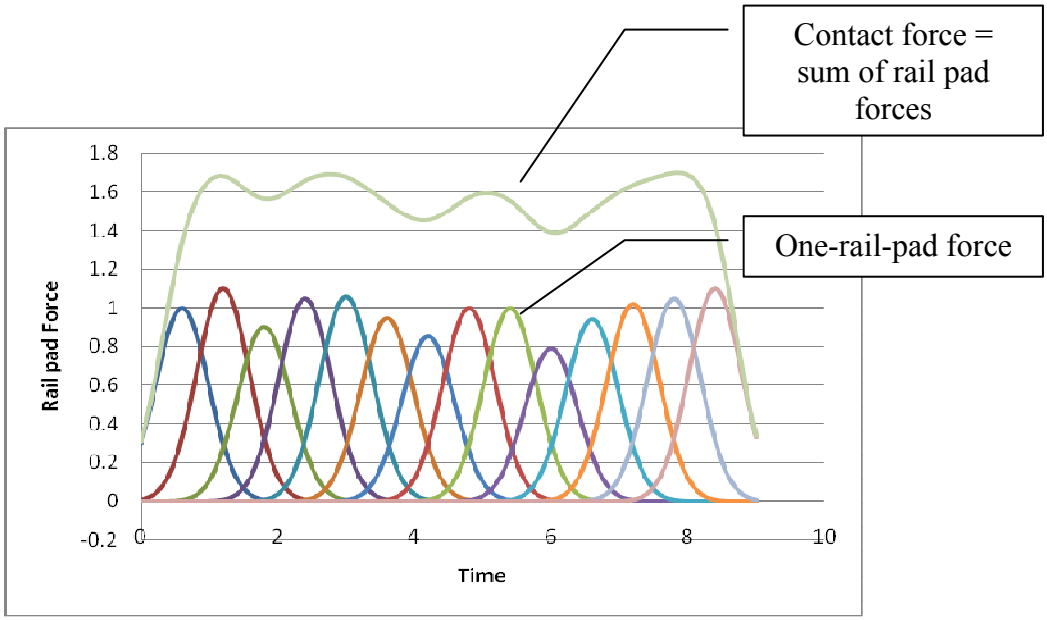

Figure 8: Rail pad force versus time and summation

The analysis of the fluctuation of the contact force over several wheel perimeters will lead to the following conclusions:

- If the force is periodic over a wheel perimeter, then the excitation is mainly due to the wheel surface. Low and high roughness wheels can be distinguished
- If the force does not show any periodic behaviour, then the main excitation comes from the track.

The calculated contact force can be used as an input for computations.

Measurement of the track stiffness by standstill methods using RSMV

Instead of using the pass-by of regular trains for the excitation generation, the standstill method for the track stiffness measurements can also be performed by using the RSMV as the source of vibration. This has the advantage that the static and dynamic excitation forces are measured. Moreover, the excitation can be controlled between 0 and 20 Hz.

Measurement of track stiffness by continuous methods

No specific protocol is described here, but the chosen measurement method must give the track stiffness variation along track.

The measurement conditions must be reported:

- Description of measurement vehicle used
- Measurement vehicle speed
- Frequency range of measurements
- Site description

The results should be presented as the stiffness along track for each frequency of measurement.

The specific requirements for the instrumentation are:

- The minimum measurable deflection should be below 0.1 mm
- The sampling should allow to have at least 4 points between 2 adjacent sleepers (at least a measurement point about every 15 cm)

Figure 9 gives an example of expected measurement result (by Trafikverket, RSMV).

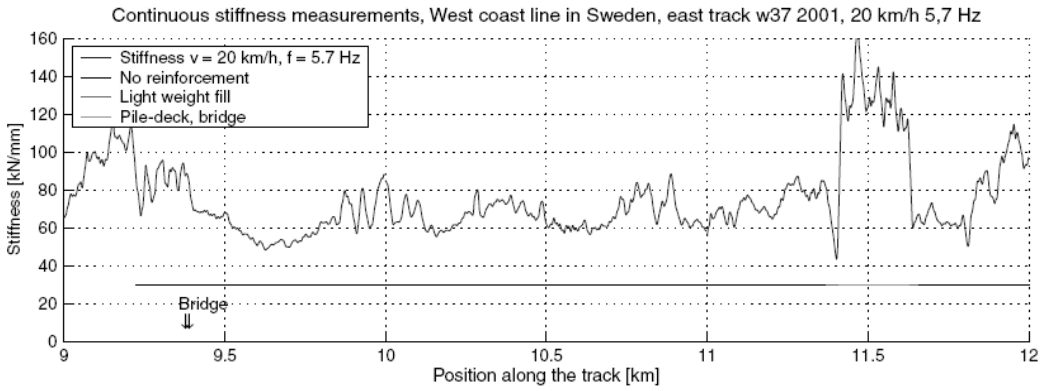

Figure 9: Track stiffness measurement for crossing a bridge [9]

3.3 SOIL CHARACTERIZATION

3.3.1 General aspects

Accurate assessment of railway induced vibrations and the efficiency of vibration mitigation measures requires detailed knowledge of the transfer functions between the track and the free field and the track receptance. Both are influenced by the dynamic soil characteristics.

This section summarizes the measurement protocol within RIVAS to determine dynamic soil characteristics and transfer functions in the free field and from the track to the free field.

3.3.2 Dynamic soil characteristics (for calculating H and A_R)

Assumptions

In deliverable D1.1 "Test procedures for the determination of the dynamic soil characteristics" of the RIVAS project [10], the following assumptions have been formulated regarding the constitutive behavior of the soil as well as the modeling of wave propagation in the soil:

1. The dynamic (axle) loads remain of relatively low amplitude so that small strain levels in the order of magnitude 10^{-6} – 10^{-5} prevail and linear elastic constitutive behavior can be assumed in the soil.
2. The soil can be represented as a horizontally layered elastic halfspace, where the material properties only vary in the vertical direction.
3. The constitutive behavior of the soil is assumed to be isotropic in each layer. Anisotropic constitutive behavior would better represent the geological formation process, but is generally not accounted for in geophysical prospection methods and state-of-the-art models.
4. Six parameters need to be determined for each layer: the layer thickness d, the shear and dilatational wave velocities c_s and c_p, the material damping ratios β_s and β_p in shear and dilatational deformation, and the mass density ρ. The underlying halfspace is characterized by five parameters. It is often assumed that the material damping ratios β_s and β_p are equal.
5. The depth up to which these parameters should be investigated depends on the lowest frequency of interest and the stiffness of the soil.

Recommended course of action

Deliverable D1.1 of the RIVAS project [10] has identified test procedures for the determination of the dynamic soil characteristics, based on classical laboratory tests, seismic in situ tests and dynamic laboratory tests. Deliverable D1.1 proposes the following course of action to determine dynamic soil characteristics, accounting for feasibility and available budget within the RIVAS project:

1. Study of archive records (geological maps, …) and geotechnical investigations (drillings, samplings, laboratory tests, in situ tests, …). Soil layering and dynamic soil characteristics can be estimated from empirical relations between classical soil mechanics parameters and dynamic soil characteristics. Within RIVAS, however, this cannot replace determination of dynamic soil characteristics by means of in situ and laboratory tests.
2. Laboratory tests on (undisturbed) soil samples to determine the mass density ρ and other parameters such as void ratio, degree of saturation, … Based on these parameters, empirical relations can provide an update of the estimated dynamic soil characteristics. At least one sample per soil layer is recommended; due to the heterogeneous nature of the soil, it is highly recommended to take samples at different lateral positions as to obtain spatially averaged values per soil layer.
3. Seismic in situ tests on a representative volume of soil in natural stress and compaction conditions at small strain levels. A (non-invasive) combined surface wave - seismic refraction test is proposed as it is easy to perform at relatively low cost and allows to determine all required dynamic soil characteristics. Disadvantages may be lack of penetration depth and resolution.
4. Additional borehole methods (down-hole, cross-hole, …) or a SCPT can be performed, as to provide better spatial resolution up to larger depth.
5. Dynamic laboratory tests on undisturbed samples, such as the resonant column test and the cyclic tri-axial test (combined with bender element measurements), may be used to determine the (shear) strain dependency of the shear modulus and material damping ratio.

Steps 1-3 are minimum constituents of a reliable soil investigation campaign within the RIVAS project. The use of borehole methods (step 4) is highly recommended if budget is available. Laboratory tests (step 5) are useful to verify the assumption of linear behavior and to gain insight in non-linear effects close to the source of vibration. They can, however, not replace in situ testing.

The results of the soil investigation campaigns need to be reported in a detailed (and reproducible) manner, containing information about the study of archive records, the soil sampling, the (classical) laboratory tests, the seismic in situ tests and the dynamic laboratory tests. The results should be summarized, providing soil profile(s) including the following information for each layer: the layer thickness d, the wave velocities C_s and C_p, the material damping ratios β_s and β_p and the mass density ρ. It is also advisable to report on the validation of the test results (e.g. comparing measured and computed transfer functions in the free field), in order to provide an indication of the reliability of the obtained dynamic soil characteristics.

Spectral analysis of Surface Waves test

The Spectral Analysis of Surface Waves (SASW) test is a well-established non-invasive test method to determine the (small strain) shear modulus [11,12]. The SASW method has been used to investigate pavement systems [13], to assess the quality of ground improvement [14], to determine the thickness of waste deposits [15], and to identify the dynamic soil properties for the prediction of ground vibrations [3,16-17]. The SASW method has more recently also been applied to determine the material damping ratio [18-22]. The SASW method consists of three steps:

1. An in situ measurement is performed where surface waves are generated by means of an impact hammer, a falling weight, or a hydraulic shaker. The wave field is recorded by accelerometers or geophones along a straight measurement line on the soil's surface.
2. The experimental dispersion curve $C_R^E(\omega)$ and attenuation curve $A_R^E(\omega)$ (i.e. the phase velocity and the attenuation factor as a function of the frequency ω) are determined from the measurement data. Different procedures can be used, as will be discussed further.
3. An inverse problem is formulated as a constrained optimization problem and solved in order to find a soil profile corresponding to the experimental dispersion and attenuation curves.

In situ experiment

The SASW method relies on the measurement of surface waves, which propagate in the horizontal direction and decay exponentially with depth. For low frequencies, the wavelength of the surface waves is large and the surface waves reach deep soil layers. These layers are generally stiff and weakly damped, resulting in a high phase velocity and a low attenuation coefficient. For high frequencies, the wavelength of the surface waves is smaller and the surface waves travel through shallow soil layers. These layers are generally softer and more strongly damped, resulting in a lower phase velocity and a higher attenuation coefficient. As a consequence, the phase velocity and attenuation coefficient of surface waves vary with the frequency and are determined by the variation of the soil properties with depth.

Instead of using harmonic excitation, it is much more efficient to simultaneously exciting different frequencies by means of transient excitation. Different sources can be used, such as an impact hammer, a falling weight, or a hydraulic shaker. The strains in the soil should remain limited to strain levels occurring in railway induced vibration problems. Good experience has been obtained with the following excitation sources:

- An instrumented impact hammer, e.g. a PCB impact hammer with a mass of 5.5 kg, equipped with a relatively soft tip (that can be replaced with a harder tip) and a force sensor (figure 10a). The impacts are applied on an aluminum or steel foundation on the soil's surface [23], e.g. on a 40 cm x 40 cm x 8 cm aluminum foundation. Four aluminum stakes with a length of 20 cm are connected to the bottom of this foundation in order to ensure good contact with the soil during impact.
- A falling weight device, e.g. with a modular mass of maximum 120 kg falling from a height of maximum 0.9 m (figure 10b). The impacts are applied on a modular steel foundation on the soil's surface. The mass falls on a dashpot mounted on the steel foundation, preventing rebound after impact. Three force sensors are installed between the bottom plate of the dashpot and the steel foundation to measure the impact force.
- A hydraulic shaker, e.g. an XCITE 1100 system with a Zonic exciter head ES301, with a peak dynamic force of about 4.4 kN in the frequency range between 25 and 100 Hz (figure 10c). This shaker is mounted on a modular steel foundation on the soil's surface and equipped with a load cell. The shaker can be controlled as to apply, for example, harmonic and swept sine signals.

Figure 10: SASW test setup with (a) an impact hammer, (b) a falling weight, and (c) a hydraulic shaker.

The input force must be measured so that the free field transfer functions are available; these are needed for the determination of the material damping ratio and for a validation by comparing the measured and computed (based on the identified dynamic soil characteristics) transfer functions.

Furthermore, the vertical response of the foundation is measured using four accelerometers installed at its corners as to determine the vertical foundation impedance.

In order to obtain a high coherence over a wide range of frequencies, different sources can be used. Each source is rich in certain frequencies so when multiple sources are used, a broad bandwidth is excited.

The wave field in the soil is recorded by a (large) number of seismic accelerometers with high sensitivity (e.g. 10 V/g) and low resolution (e.g. below 8 μg), that are placed along a straight measurement line along the soil's surface in a common source-receiver setup. Alternatively, a string of geophones may be used. The vertical component is usually measured, although the horizontal component parallel to the measurement line can also be used. Good coupling of the sensors to the ground is crucial. Several mounting methods for accelerometers have been investigated (e.g. on an aluminum block, on steel or aluminum stakes); good results have been obtained mounting an accelerometer on an aluminum stake with a length of 30 cm and a cruciform cross section as to minimize dynamic soil-structure interaction effects.

The number of sensors is strongly related to the method to determine the experimental dispersion and attenuation curves, as will be explained in the following subsection.

1. The oldest and most basic method employs harmonic excitation and a single or two-receiver setup.
2. A more efficient estimate of the surface wave velocity is obtained by means of Nazarian's method [11], where an impulsive source and a line of multiple receivers are used. The wave velocities are estimated from the phase of the transfer functions between (different) pairs of receivers. A recommended receiver positioning scheme is

to place the first sensors at 2 and 3 m from the source and then use multiples of these distances for the other sensors (e.g. 2 m, 3 m, 4 m, 6 m, 8 m, 12 m, 16 m, 24 m, 32 m, 48 m, 64 m)

3. The third method, which also uses an impulsive load and multiple receivers, is based on the transfer function $\hat{H}(r,\omega)$ between the impact force and the vibrations at the receivers at distance r from the source [24, 25]. Most recent methods are based on a transformation of the transfer function $\hat{H}(r,\omega)$ to the frequency-wavenumber domain. In order to obtain a good spatial resolution, a dense receiver setup (e.g. 100 equidistant receivers, located up to 100 m from the source) is preferred. If only a limited number of receivers is available, several setups with different receiver positions can be measured consecutively (e.g. a first setup with 10 receivers at 1, 11, …, 91 m followed by a second setup with 10 receivers at 2, 12, …, 92 m, …). Results obtained with this measurement setup can also be interpreted as a seismic refraction test.

Wave velocities and attenuation curves are estimated from the transfer functions between pairs of receivers or between source and receiver. The H_1-estimator of the transfer function is used for this purpose [26]. Assuming that the noise fulfills the conditions stated by the central limit theorem, the accuracy of the estimator increases proportionally to $\sqrt{N}$, with N the number of events recorded (e.g. hammer impacts). Practical experience with impact hammer tests has demonstrated that qualitative results are obtained with a relatively high number $(N \geq 100)$ of impacts. Most of the experiment time goes into the set-up of the receivers, while recording multiple impacts does not cost a lot of extra time. It is therefore recommended to record at least 20 times. SASW tests with 100 repetitions are not uncommon.

Data acquisition should be performed using an analog anti-aliasing filter or at a sufficiently high sampling rate (over-sampling); digital data can subsequently be resampled at a lower sampling frequency using a digital anti-aliasing filter with a variable cut-off frequency. Accounting for the frequency input of the excitation, a sampling frequency of 1000 Hz and a corresponding Nyquist frequency of 500 Hz is sufficiently high. The number of samples or the signal period T should be sufficiently high so that both, the information prior to the impact (pre-trigger) as well as all relevant vibrations after the impact (post-trigger) are included in the recordings, properly accounting for wave propagation and attenuation in the soil. The signal period should also be high enough as to obtain a sufficiently low frequency bin $\Delta f = 1/T$.

Determination of the experimental dispersion and attenuation curve

The second step in the SASW method involves the determination of the experimental dispersion curve $C_R^E(\omega)$ and attenuation curve $A_R^E(\omega)$ (i.e. the phase velocity and the attenuation factor as a function of the frequency) from the measurement data. Different procedures can be used to determine the experimental dispersion curve $C_R^E(\omega)$. The third method also allows determining the attenuation curve $A_R^E(\omega)$ and, consequently, the material damping ratio.

1. The oldest and most basic method is to apply a steady-state harmonic force with frequency f on the surface and use a receiver to find the distance to the nearest point that moves in phase with the excitation source. The distance between the source and

the receiver is then assumed to equal one wavelength λ. The wave velocity C_R^E is calculated as $f\lambda$. Performing this experiment for various frequencies provides the data required to find the experimental dispersion curve. Compared to the following methods, this method is inefficient and not recommended.

2. A more efficient estimate of the surface wave velocity is obtained by means of Nazarian's method [11], where an impulsive source and a line of multiple receivers are used. The wave velocities are estimated from the phase of the transfer functions between pairs of receivers. The H_1-estimator of the transfer function is used for this purpose [26]. For each receiver pair, the phase velocity of the surface wave is estimated as $C_R^E(\omega) = \omega \Delta r_{ij} / \theta_{ij}(\omega)$, where Δr_{ij} is the distance between the receivers and $\theta_{ij}(\omega)$ is the unfolded phase of the transfer function. The results for each receiver pair are withheld for a certain frequency only if the coherence between the signals is sufficiently high [27] and the measured wavelength λ_R^E is not too high or too low compared to the receiver pair distance Δr_{ij}. The lower bound $\bar{r}_{\min}$ for the ratio $\Delta r_{ij}/\lambda_R^E$ acts as a high-pass filter $(f \geq \bar{r}_{\min} C_R^E / \Delta r_{ij})$ that limits the contribution of body waves, while the upper bound $\bar{r}_{\max}$ serves as a low-pass filter $(f \leq \bar{r}_{\min} C_R^E / \Delta r_{ij})$ to remove the high frequency components contaminated by coherent noise [11]. Because of these thresholds, it is recommended to use different receiver pair distances. A recommended receiver positioning scheme is to place the first sensors at 2 and 3 m from the source and then use multiples of these distances for the other sensors, as explained in the previous subsection. The lowest distance determines the highest measurable frequency, while the largest distance determines the lowest measurable frequency and therefore the depth to which can be measured. This puts a minimum limit on the distance of the farthest separated receiver pair. The dispersion curves of the different pairs are finally combined by fitting a high order polynomial to the cloud of points obtained from all pairs.

   Nazarian's method can be adjusted for use in a passive SASW, for which no excitation source is needed and ambient vibrations are used instead [28]. These passive SASWs are suitable to measure in a low frequency range [29].

3. The third method, which also uses an impulsive load and multiple receivers, is based on the transfer function $\hat{H}(r, \omega)$ between the impact force and the vibrations at the receivers at distance r from the source [24, 25]. Most recent methods are based on a transformation of the transfer function $\hat{H}(r, \omega)$ to the frequency-wavenumber domain. The resulting frequency-wavenumber spectrum $\hat{H}(k_r, \omega)$ exhibits peaks corresponding to the occurrence of the surface waves. The positions of the peaks reveal the dispersion curves, while their width is used to determine the attenuation curves, using the half-power bandwidth method [30, 31].

   Other methods to determine the attenuation curve exist, such as phase and amplitude regression in the frequency-space domain [20], but are based on the hypothesis that the response of the soil is due to a single surface mode [22, 18, 19].

   In a similar way as for the previous methods, the inter-receiver distance and the array length determine the shortest and longest measurable wavelength and, consequently, the frequency range where the dispersion and attenuation curves can be determined. The number of receivers determines the accuracy of the frequency-wavenumber spectrum. If only the dispersion curve is of interest, it is suggested to use the same

setup as for the method based on receiver-pair transfer functions. This approach gives a relatively rough approximation of the frequency-wavenumber spectrum, but it is sufficiently fine to determine the positions of the peaks in an accurate way. If the attenuation curve needs to be determined as well, a higher number of receivers is required (e.g. 30 to 100 instead of 10), so that the shape of the peaks is resolved sufficiently well for the application of the half-power bandwidth method.

Soil parameter estimation from measurement data

The shear wave velocity profile is finally determined from the experimental dispersion through the solution of an inverse problem. Similarly, the material damping ratio profile is determined from the attenuation curve. Both inverse problems can be solved consecutively or be formulated as a single (combined) inverse problem.

An initial profile for the shear wave velocity is estimated by approximating the experimental $C_R^E - \lambda_R^E$ curve with a stepwise function, using the approximate relations $C_s = 1.1C_R^E$ and $z = \lambda_R^E/3$. An initial profile for the material damping ratio is estimated using the approximate relations $\beta = \lambda_R^E A_R^E/2/\pi$ and $z = \lambda_R^E/3$.

The direct stiffness method [32] or an equivalent formulation is used to calculate the theoretical dispersion and attenuation curves of a soil with a given stiffness and damping profile. The ElastoDynamics Toolbox EDT [33] can be used for this purpose. The theoretical dispersion curve corresponds to the first (or fundamental) mode of a layered halfspace or to the effective dispersion curve (a combination of multiple modes) in the case of inverse layering where still layers are underlain by softer layers [34, 35].

The profile is iteratively adjusted in order to minimize a misfit function that measures the distance between the theoretical and the experimental dispersion and attenuation curves. The minimization problem is usually solved with a gradient based local optimization method [11].

The dispersion and attenuation curves are insensitive, however, to variations of the soil properties on a small spatial scale or at a large depth. The information on the soil properties provided by these curves is therefore limited. As a result, the solution of the inverse problem is non-unique: the soil profile obtained from the inversion procedure is only one of the profiles that fit the experimental data. The non-uniqueness of the solution of the inverse problem in the SASW method and the resulting impact on the accuracy of ground vibration predictions have been investigated in reference [36].

Practical applications

An application of Nazarian's method to obtain the shear wave velocity profile at the site in Lincent along the high speed track L2 between Brussels and Köln can be found in [37].

Alternative determination of the experimental dispersion curve by means of the transfer functions in the frequency-wave number domain can be found in [30, 38, 31].

Several alternatives to determine the attenuation curve and the material damping ratio profile on the same site have also been discussed in [30, 38, 31].

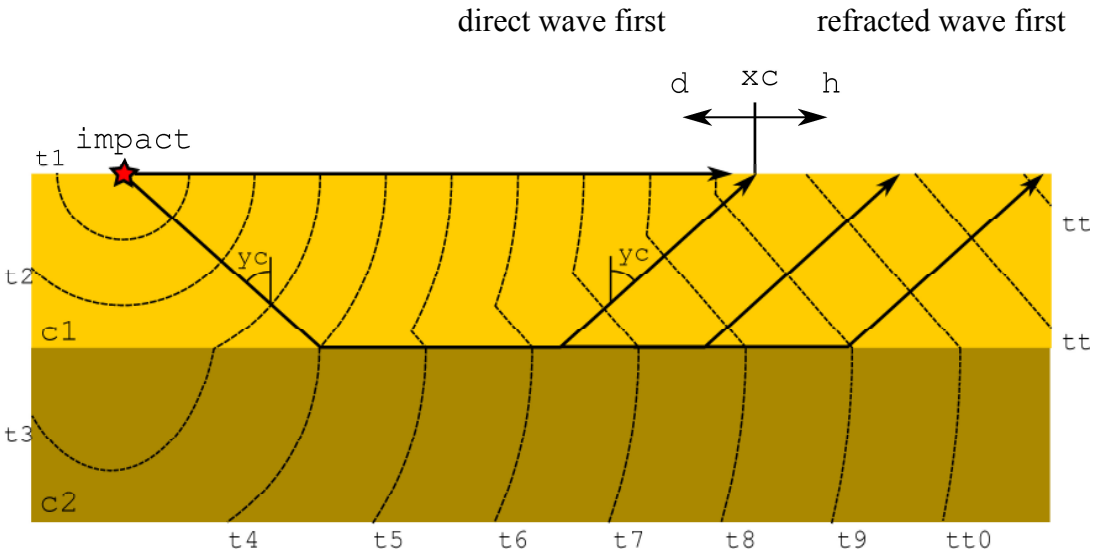

Figure 11: Seismic refraction principles. The wavefronts are represented by the dashed lines, the wave paths with the solid arrows.

Seismic refraction test

The seismic refraction method is a non-invasive test method, used for the determination of the P-wave velocity C_p and the thickness of the different layers. Seismic refraction is a phenomenon related to the directional change of a wave when it crosses an interface between two layers with different mechanical properties or P-wave velocities, described by Snell's law:

$$C_{p1} \sin\theta_1 = C_{p2} \sin\theta_2 \tag{4}$$

with C_{p1} and C_{p2} the P-wave velocities in the top and bottom layer and θ_1 and θ_2 the wave propagation directions in the top and bottom layer. The critical angle is the incident wave angle θ_1 for which the refracted wave travels horizontally $(\theta_2 = 90°, C_{p2} > C_{p1})$:

$$\theta_c = \arcsin\left(\frac{C_{p2}}{C_{p1}}\right) \tag{5}$$

An impact at the free surface results in P-waves (figure 11), initially propagating only in the top layer. At t_4, the wave with the critical angle θ_c hits the interface, which creates a critically refracted wave that travels with a velocity $C_{p2} > C_{p1}$ along the interface. This wave creates a wave that propagates upwards at an angle $\theta_c$with a velocity C_{p1}. At points along the surface close to the impact point $(x \leq x_c)$, the direct P-wave is faster than the refracted wave. At points further away from the impact point $(x \geq x_c)$, the refracted waves are faster than the direct waves.

The seismic refraction test consists of three steps:

1. An in situ measurement is performed where P-waves are generated by means of an impact hammer, a falling weight or a small explosion (in which case the impact force

remains unknown). The wave field is recorded by accelerometers or geophones along a straight measurement line on the soil's surface.

2. The experimental P-wave arrival time $T_P^E(r)$ is determined from the measurement data, e.g. based on the STA/LTA procedure.

3. An inverse problem is formulated as a constrained optimization problem and solved in order to find a soil profile corresponding to the P-wave arrival time.

In situ experiment

The seismic refraction test relies on the measurement of direct and refracted P-waves along a measurement line on the soil's surface.

An impact excitation is applied using an instrumented impact hammer or a falling weight, as outlined before. The impact force is measured using a load cell, so that transfer functions can be determined. The impact force is usually applied on a surface foundation, of which the vertical response is measured with four accelerometers installed at its corners as to determine the vertical foundation impedance. A (small) explosive source can be used alternatively, in which case the impact force remains unknown and transfer functions cannot be determined.

The wave field in the soil is recorded by a (large) number of seismic accelerometers with high sensitivity (e.g. 10 V/g) and low resolution (e.g. below 8 μg), that are placed along a straight measurement line along the soil's surface in a common source-receiver setup. Alternatively, a string of geophones can be used. The vertical component is measured. Good coupling of the sensors to the ground is required.

The number of sensors along the surface should be sufficiently large and is determined by the inter-receiver distance and the distance between the source and the furthest receiver, which determine resolution and depth of exploration, respectively. For a soil with a single layer with thickness H on top of a halfspace, the cross-over point x_c of the direct and critically refracted wave is computed as:

$$x_2 = 2H\sqrt{\frac{C_{p1} + C_{p2}}{C_{p2} - C_{p1}}} \tag{6}$$

If prior knowledge of the soil stratigraphy is available, this equation can be used to determine the sensor layout as to enable measurement of the critically refracted wave(s). In many cases, the experimental setup with a large number of receivers (e.g. 100 equidistant receivers up to 100 m from the source) as used in the third SASW method can also be used as a seismic refraction test setup; a single test can then be interpreted as a SASW test and a seismic refraction test.

In order to improve the signal-to noise ratio in the far field, stacking techniques are commonly used: a large number N of events is recorded, and the resulting time signals are added up. Assuming that the noise fulfills the conditions stated by the central limit theorem, the signal-to-noise ratio of the stacked signal improves proportionally to $\sqrt{N}$. Practical experience with impact hammer tests has demonstrated that qualitative results are obtained with a relatively high number of impacts (e.g. 100 impacts, which means that an improvement of the signal-to-noise ratio with a factor of 10 is expected with respect to the single impact experiment). Data acquisition can proceed as for the SASW test.

Determination of the P-wave arrival time

The second step in the seismic refraction method involves the determination of the experimental P-wave arrival time $T_P^E(r)$ from the stacked time signals.

A Short Term Averaging / Long Term Averaging (STA/LTA) procedure is followed in order to detect the first arrivals [39]. The STA/LTA ratio $R(r,t)$ is computed as follows:

$$R(r,t) = \frac{\frac{1}{N_S}\sum_{k=0}^{N_S-1} a^2(t-k\Delta t)}{\frac{1}{N_L}\sum_{k=N_S}^{N_S+N_L-1} a^2(t-k\Delta t)} \tag{7}$$

where N_S and N_L are the durations of two adjacent windows (a short one and a long one) in terms of samples and Δt is the sampling step.

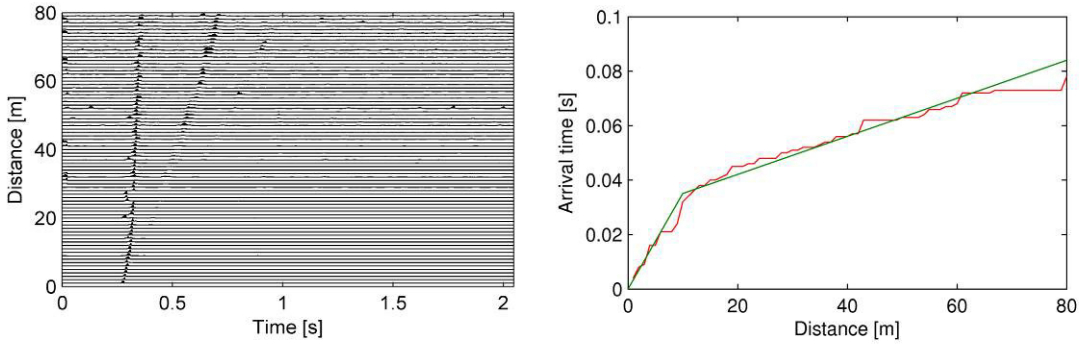

Figure 12: (a) STA/LTA ratio $R(r,t)$ of the free field acceleration (stacked for 100 hammer impacts) and (b) resulting experimental P-wave arrival time $T_P^E(r)$ (red line) and bilinear approximation (green line) at the site in Lincent.

Figure 12(a) shows the STA/LTA ratio $R(r,t)$ of the free field acceleration (stacked for 100 hammer impacts) at the site in Lincent, computed with values $N_S = 20$ and $N_L = 50$. Strong peaks occur when the short term window captures the first part of the signal while the long term window still contains only noise. These peaks reveal the experimental P-wave arrival time $T_P^E(r)$, which is determined as the time t where the STA/LTA ratio $R(r,t)$ reaches its maximum. In the near field, this procedure generally gives satisfactory results, but in the far field, spurious peaks or peaks corresponding to the arrival of the surface waves may cause errors in the identified arrival time $T_P^E(r)$. In order to eliminate these errors, the arrival time at each receiver is compared with minimum and maximum values given the arrival time at the previous receiver and a lower and upper bound for the P-wave velocity. Values C_p^{low} = 100m/s and C_p^{upp} = 2000m/s are used in the present analysis. If the arrival time is not between the minimum and maximum value, it is replaced with a value obtained by linear extrapolation of the values corresponding to the two previous receivers. Finally, the curve obtained is shifted in time to ensure that the arrival time $T_P^E(r)$ at $r = 0$ (determined by linear extrapolation) is equal to zero. The resulting experimental P-wave arrival time $T_P^E(r)$ is shown in figure 12(b). The curve can be approximated by a bilinear curve, revealing the presence of a layer with a low P-wave velocity on a halfspace with a higher P-wave velocity. The actual P-wave velocity is determined by the solution of an inverse problem.

Determination of the P-wave velocity

The P-wave velocity profile is determined from the experimental P-wave arrival time through the solution of an inverse problem. An initial soil profile is proposed based on the P-wave arrival time $T_P^E(r)$ which is manually approximated by means of bilinear curve(s) (figure 12(b)). The P-wave velocity of the layer(s) and the halfspace follow from the slopes of this curve, while the thickness of the layer(s) is determined from the location of the intersections. The corresponding theoretical P-wave arrival time is computed and compared with the experimental curve. The soil profile is iteratively adjusted in order to improve the fit between the theoretical and experimental curves.

Practical applications

A seismic refraction test on the site in Lincent along the high speed track L2 between Brussels and Köln has been discussed in [38].

Combined SASW and seismic refraction test

It follows from the two previous subsections that a seismic in situ test involving an impact load on a surface foundation and a large number of closely spaced receivers along a measurement line on the soil's surface can be interpreted both as an SASW and a seismic refraction test.

Within the context of the SASW test, the time histories of the acceleration measured at different locations as well as the measured impact force are used to derive the transfer functions in the frequency-wavenumber domain, allowing to determine the experimental dispersion curve $C_R^E(\omega)$ and attenuation curve $A_R^E(\omega)$ (i.e. the phase velocity and the attenuation factor as a function of the frequency).

The same test can be interpreted as a seismic refraction test, where the experimental P-wave arrival time $T_P^E(r)$ is determined from applying a STA/LTA procedure on the stacked time histories.

The initial soil profile (S-wave velocity, P-wave velocity and material damping ratio) is determined based on the experimental dispersion curve, attenuation curve and P-wave arrival time, as discussed in the previous subsections, and used as a starting point. The fit between the theoretical and experimental P-wave arrival time and dispersion and attenuation curves is further improved by solving an inverse problem where the misfit between these curves is minimized. A single (or combined) inverse problem is solved, taking into account the three curves simultaneously.

The design variables in the optimization scheme are the layer thicknesses d, the shear wave velocities C_s, the ratio $s = C_s/C_p$ of the shear and dilatational wave velocities, and the material damping ratios β_s and β_p. The density is kept fixed during the inversion procedure. Inequality constraints are defined on all design variables defining the range of allowable values. Weighting factors determine the relative contribution to the objective function of the misfit for the P-wave arrival time, the dispersion curve, and the attenuation curve, respectively.

The optimization problem is a nonlinear least-squares problem; it is solved, for example, by means of the MATLAB function lsqnonlin, which is based on a trust-region-reflective

algorithm. This algorithm is a subspace trust-region method and is based on the interior-reflective Newton method [40].

The combined inversion of the P-wave velocity, S-wave velocity and material damping ratio based on a seismic refraction and SASW test on the site in Lincent along the high speed track L2 between Brussels and Köln has been discussed [38].

Soil under the track

The soil below the track and subgrade is usually assumed to have the same layering and dynamic soil characteristics as in the free field.

Repeated axle loads may have resulted in a densification of the soil under the track, however, revealing higher values of dynamic stiffness. In order to determine the dynamic characteristics of the soil (and the subgrade layers) under the track, in situ seismic tests (e.g. an SASW test) can be performed with a measurement line along the track. The excitation (e.g. using an instrumented impact hammer) can be applied in the middle of a sleeper, while the (vertical) response is measured with accelerometers fixed on several sleepers; the number and distance between accelerometers can be determined according to the guidelines defined in the previous subsections.

Whereas the experimental setup is straightforward and poses no particular problems, the solution of the inverse problem to infer the dynamic characteristics of the subgrade and soil layers is more difficult. For the forward modeling in the inverse problem, a numerical model incorporating the track, the subgrade layers and the layered soil must be used (e.g. involving a coupled finite element-boundary element model of the track-soil system); this is computationally more demanding than a layered soil model. Furthermore, as the track and subgrade layers may be stiffer that the underlying soil, higher modes may dominate the response along the track.

The application of the SASW method along a track is a very interesting matter of ongoing research. Within the frame of the RIVAS project, it is suggested to use the same layering and dynamic soil characteristics below the track as determined in the free field.

3.3.3 Transfer function *H*

Transfer functions in the free field

Transfer functions in the free field are determined by means of loading (e.g. instrumented impact hammer, falling weight, shaker) on a foundation. The force must be measured by means of a load cell. The vertical response of the foundation is measured using four accelerometers at its corners as to determine the vertical foundation impedance.

The wave field in the soil is recorded by seismic accelerometers with high sensitivity and low resolution or geophones that are placed at the soil's surface in a common source-receiver setup. Alternatively, a string of geophones may be used. Accelerometers should at least be placed at 8 m, 16 m, 32 m, and 64 m from the source, while additional positions at 2 m, 3 m, 4 m, 6 m, 12 m, 24 m, and 48 m (or more) are welcome. In these points, the vertical component should be measured, while the horizontal (radial) component can also be of interest. Good coupling of the sensors to the ground is crucial.

The number of impacts N should be sufficiently large as to improve the signal-to-noise ratio. The measurement setup, data acquisition and signal processing procedure are similar as for the SASW and seismic refraction test outlined before.

The average transfer function $\hat{H}_{ij}(\omega)$ from the impact force (channel i) to the free field response at a distance r (channel j) is determined using the H_1-estimator [26]:

$$\hat{H}_{ij}(\omega) = \frac{\hat{S}_{ij}(\omega)}{\hat{S}_{ii}(\omega)} \tag{8}$$

The average cross power spectral density $\hat{S}_{ij}(\omega)$ of channels i and j for N impacts is computed as:

$$\hat{S}_{ij}(\omega) = \frac{1}{N}\sum_{k=1}^{N} \hat{x}_i^k(\omega)\hat{x}_i^{k*}(\omega) \tag{9}$$

Where $\hat{x}_i^k(\omega)$ is the frequency content of the signal recorded in channel i for impact k and $\hat{x}_i^{k*}(\omega)$ is the complex conjugate of $\hat{x}_j^k(\omega)$.

The transfer function $\hat{H}_{ij}(\omega)$ obtained with the H_1-estimator is a random variable, as each experiment gives rise to a different estimation. The estimated transfer function $\hat{H}_{ij}(\omega)$ can therefore be characterized by a variance $\hat{\sigma}^2_{H_{ij}}(\omega)$. Assuming that the noise is stationary, the variance $\hat{\sigma}^2_{H_{ij}}(\omega)$ is computed as [41]:

$$\hat{\sigma}^2_{H_{ij}}(\omega) = \frac{1-\hat{\gamma}^2_{ij}(\omega)}{N\hat{\gamma}^2_{ij}(\omega)}\left|\hat{H}_{ij}(\omega)\right|^2 \tag{10}$$

where $\hat{\gamma}_{ij}(\omega)$ denotes the coherence between channels i and j:

$$\hat{\gamma}^2_{ij}(\omega) = \frac{\hat{S}_{ij}(\omega)\hat{S}^*_{ij}(\omega)}{\hat{S}_{ii}(\omega)\hat{S}^*_{jj}(\omega)} \tag{11}$$

Assuming that the estimated transfer function $\hat{H}_{ij}(\omega)$ follows a Gaussian probability distribution, its modulus follows a Rice distribution [42]. The bounds of the confidence interval that contains the modulus with a probability p are computed as the inverse cumulative Rice distribution evaluated at $(1-p)/2$ and $(1+p)/2$.

The determination of transfer functions in the free field on the site in Lincent along the high speed track L2 between Brussels and Köln is discussed in [43, 44].

Transfer functions between the track and the free field

Transfer functions between the track and the free field are determined by means of loading (e.g. instrumented impact hammer, falling weight, shaker) on the rail (at a sleeper position) or the sleeper of the track. The force must be measured by means of a load cell. The vertical response of the rail and the sleeper is measured, at the impact position (and other nearby positions if possible). As many track components (e.g. rail pads and under sleeper pads) have a dynamic stiffness that depends on the pre-load, it is desirable to preload the track corresponding to the total static load of boogie or train carriage (e.g. if mitigation measures in the track have been installed).

The wave field in the soil is recorded by seismic accelerometers with high sensitivity and low resolution or geophones that are placed at the soil's surface on a measurement line perpendicular to the track. Alternatively, a string of geophones may be used. Accelerometers

should at least be placed at 8 m, 16 m, 32 m, and 64 m from the center of the loaded track, while additional positions (e.g. at 6 m, 12 m, 24 m, and 48 m) are welcome. In these points, the vertical component should be measured, while the horizontal (radial) component can also be of interest. Good coupling of the sensors to the ground is crucial.

The number of impacts N should be sufficiently large as to improve the signal-to-noise ratio.

The measurement setup, data acquisition and signal processing procedure are similar as for the SASW and seismic refraction test outlined in the previous section.

Transfer functions are computed according to the procedure outlined in the previous paragraph.

The determination of transfer functions between the track and the free field on the the high speed track L2 in Lincent between Brussels and Köln is discussed in [43, 44].

3.4 TRACK CHARACTERIZATION

3.4.1 General aspects

Track components strongly influence the efficiency of mitigation measures at source, at track, at vehicle and in propagation path. Therefore the track receptance - defined as the rail displacement divided by the input force on the rail - is an essential parameter also for the recalculation of mitigation-measure efficiencies. Besides using the direct measurement method as roughly described in section 3.4.2, the track receptance can be calculated by using the stiffness and damping of the resilient elements and the masses involved. The measurement procedure to determine stiffness and damping parameters of resilient elements in laboratory is described in section 3.4.3. For the stiffness and the damping of the ballast, only an indirect method based on the measurement of the track receptance is presented in section 3.4.4.

3.4.2 Track receptance A_R

The track receptance describes the track dynamic behaviour. The measurement protocols are various, differing by the excitation (impact hammer, harmonic load, train pass by), and also by the track conditions (loaded or not loaded).

The conditions of measurement with regard to the real conditions give an assessment of the validity of the results. Various measurement protocols exist:

- Train pass by measurements: instrumentation using strain gauges and accelerometers on the rail
- Harmonic load with an amplitude comparable to the amplitude generated during a train pass by, with static preload (train at proximity or uncoupled mass)
- Harmonic load or impact hammer (e.g. if the excitation amplitude is low compared to a train pass by) without preload

The robustness of the measurements mainly depends on the non-linear behaviour of the elements in the track. If the track is non-linear, then the condition of measurements must be as close as possible to the real conditions.

The loaded track will have a lower receptance than the unloaded one.

Figure 13 gives the theoretical track receptance expressed as the rail displacement divided by the input force on the rail as a function of frequency. Notice that the model does not include the soil dynamics (rigid soil assumption). Several resonances are visible:

- The rail and sleeper resonance on the ballast stiffness (f_1 ~ 100 Hz on the example)
- The sleeper antiresonance (f_a ~ 300 Hz on the example)
- Uncoupling of the rail from the sleeper (f_2 ~ 600 Hz on the example)
- The pinned-pinned frequency around 1200 Hz on the example
- The rail section deformation mode above 4000 Hz

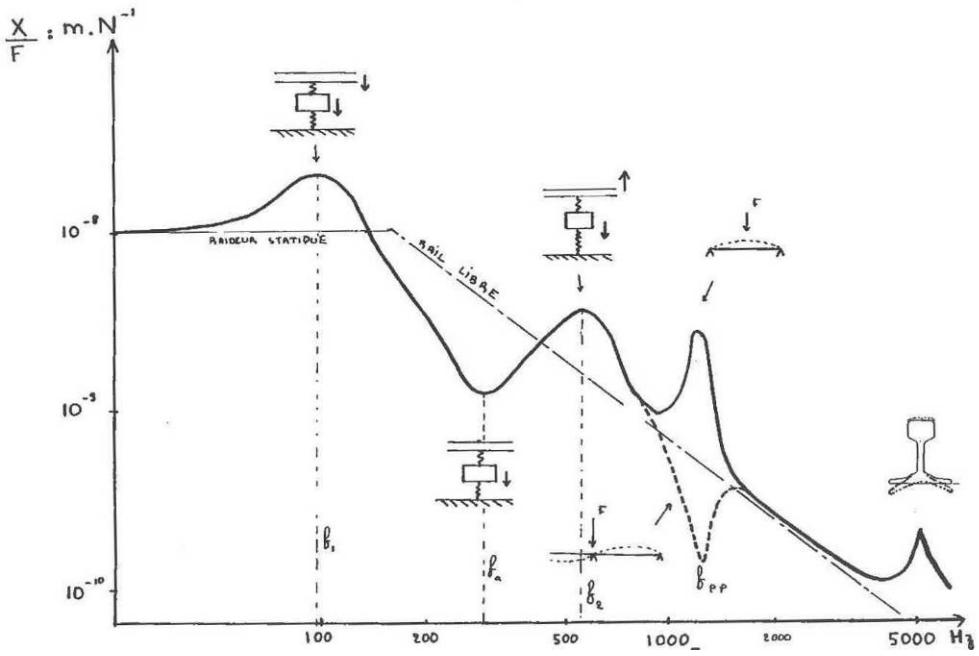

Figure 13: Rail receptance (theoretical model)

With a loaded track, the frequency f_a will be hardly visible, because loaded tracks are more damped.

When the soil has low frequency resonances, the rail receptance will differ, as illustrated in Figure 14. The peak measured at 80 Hz is due to soil resonance, which is underestimated at 25 Hz in numerical results (because of simplification in the model, such as the absence of sub-ballast). The peak at 350 Hz is the resonance of the rail on the rail pads and ballast stiffness (f_2).

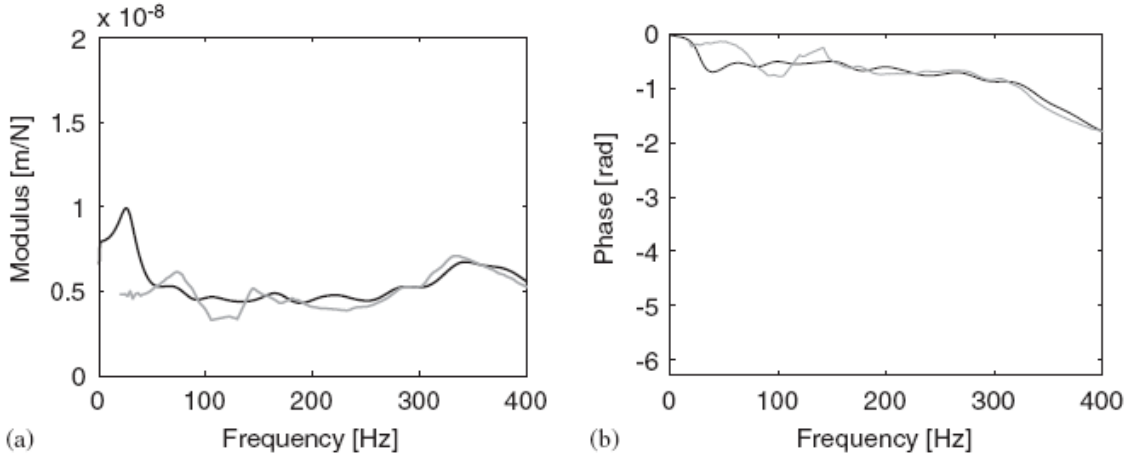

Figure 14: Rail receptance measured (grey) and calculated (black) [3]

Measurement methods to detect the track receptance are the same as described in section 3.2.4 for the measurement of track stiffness variation along the track. More information on the measurement procedures can be found in [8].

3.4.3 Stiffness and damping of resilient elements (for calculating H and A_R)

The method described in section 3.4.2 gives a global characterization of static and dynamic values of the whole track as a system. For the use within analytical models e.g. for the prediction of mitigation-measure efficiencies or for parameter studies it is vital to determine also the specific static and dynamic characteristic values of each major component within the track construction itself.

These static and dynamic properties should be determined within standardized laboratory test procedures. However, differences in the test conditions and constraints can mean that the parameters from tests at the track and those from laboratory tests do not always agree.

The most significant values according the definitions given in DIN 45673 “Mechanical vibration - Resilient elements used in railway tracks” [45] are:

- The static stiffness c_{stat} or bedding modulus C_{stat} as force (stiffness) or pressure (bedding modulus) per unit deflection is measured under a uniaxial quasi-static force.
- The dynamic stiffness $c_{dyn}(f)$ (or bedding modulus $C_{dyn}(f)$) is measured under a force in the frequency range above 1 Hz. Here, the force (for determining the stiffness) or pressure (for determining the bedding modulus) per unit deflection are obtained under a harmonically varying cyclic uniaxial force with a distinction made between: the low-frequency dynamic stiffness $c_{dyn\,1}(f)$ which is used for determining track dynamics (measured without preload, frequencies generally used are: 5 Hz, 10 Hz, 20 Hz, 30 Hz) and the higher frequency dynamic stiffness $c_{dyn\,2}(f)$ for describing the effectiveness in damping structure-borne noise (measured with preload, frequencies generally used are: 10 Hz to 160 Hz in octave intervals).
- The damping coefficient d as proportionality factor expresses the linear dependence between the damping force $F_d(t)$ and the particle velocity in the vibrating medium $v(t)$: $F_d(t)=d\cdot v(t)$.

  As a result of non-linear effects, the damping coefficient generally depends on the preloading force and on the amplitude of the particle velocity.
- The loss factor $\eta(f)$ is the ratio of the energy dissipated Q to the energy expended U for a quasistatic or harmonic load:

  $$\eta(f)=\frac{Q}{U}$$

  The loss factor is generally frequency dependent. As a result of non-linear effects, the loss factor is generally also dependent on the preloading force and on the amplitude of the velocity.

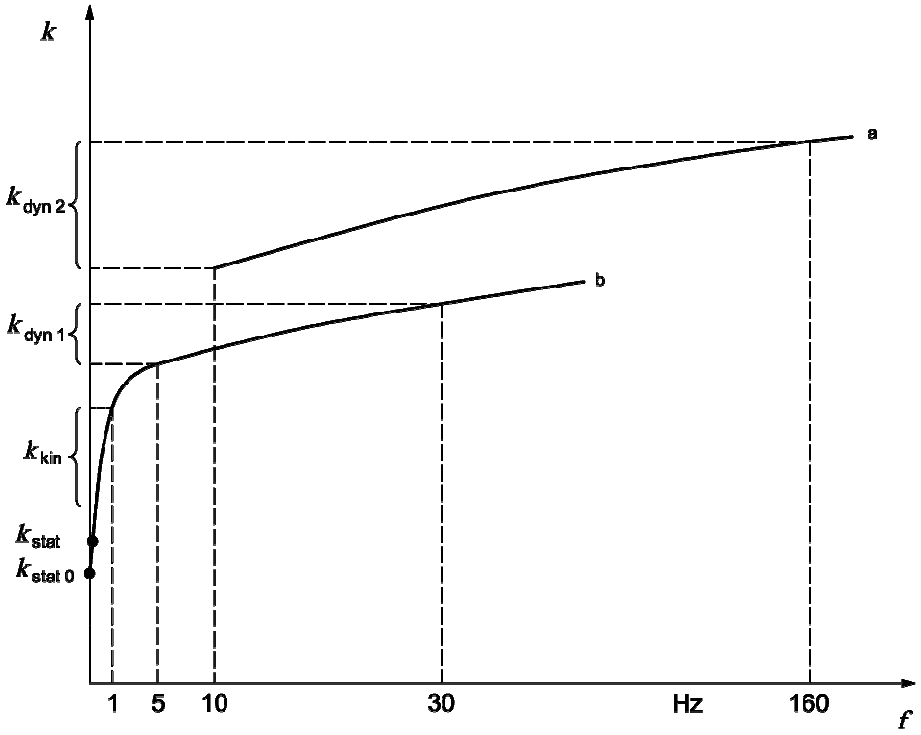

Figure 15 (DIN 45673-1 [45])**:** Stiffness curve with and without a preloading force determined in accordance with the test procedures in this standards series (schematic representation) with frequency *f* and stiffness *k*.

a Determined for a certain particle velocity and a preloading force, which determines the position of this branch of the graph

b Determined for a certain excitation force and no preloading force

The static stiffness (or static modulus) is generally determined as secant stiffness of a load/deflection diagram per unit area when a force F is applied to a continuous resilient element of area A ($\sigma = F/A$).

For the determination of the dynamic stiffness (particular for the high frequency dynamic c_{dyn2}), measurements should be performed according the guidelines within EN ISO 10846 [46]. Part 1 of this standard gives some principles and general remarks. Within the RIVAS project, the determination of the dynamic stiffness of resilient elements should be performed using the so called “direct method” as defined in part 2 of the EN ISO 10846-2 standard. Figure 16 shows the principle arrangement of the test device.

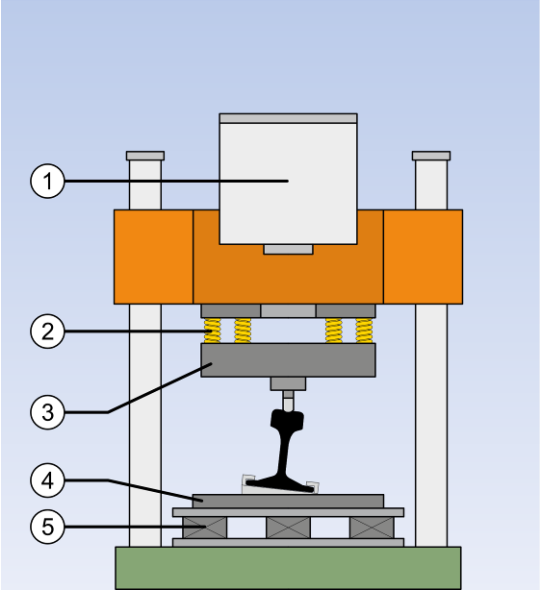

Figure 16: Principle arrangement of test procedure for the determination of the dynamic transfer properties of resilient elements, according the direct method of EN ISO 10846-2 with 1: electrodynamic vibration generator, 2: Device for decoupling the static preload, 3: Preload unit for the superposition of static and dynamic loads, 4: load measurement platform, 5: resilient layered terminating mass (figure source MÜLLER-BBM GmbH).

Stiffness and damping of the rail pad

The determination of static and dynamic properties of resilient fasteners (as an assembled system) or resilient rail pads alone should be carried out according the guidelines given in EN 13146-9 [47].

For resilient rail fasteners the requirements in the current prenorm ENV 13481-6 [48] should be considered.

Stiffness and damping of the under-sleeper pad

The determination of stiffness and dynamic properties of under-sleeper pads (USP) has to be carried out according the instructions given within DIN 45673-6 [45].

For the determination of the static and dynamic stiffness the USP-material has to be mounted on a concrete block (300 mm x 300 mm x 20 mm) instead of the concrete sleeper. The bonding layer between the concrete block and the pad shall correspond to that between a concrete sleeper and the pad. The load of the testing device shall be applied to the concrete block with the resilient element located beneath the block and on top of a profiled loading plate (NSP) whose face with the ballast profile is in contact with the pad.

For the main-line railways as considered within RIVAS the stiffness should be defined as a secant stiffness between $\sigma_1 = 0.01$ N/mm^2 to $\sigma_2 = 0.10$ N/mm^2.

Advisory Notes:

- In product data sheets of suppliers sometimes other definitions of the secant are given. These should be recalculated to the definition given in the text according to DIN 45673-6.
- Currently a European standard for Under Sleeper Pads is in preparation. Most probably the blocks required by the CEN standard will be smaller (250 mm x 250 mm x 10 mm) and a load plate with a symmetric arrangement of pyramids should be used. Using the bigger concrete blocks according DIN 45673-6 allows later on to carry out the tests also under the CEN definitions without losing the reference to former standards.

3.4.4 Stiffness and damping of the ballast (for calculating H and A_R)

Stiffness and damping of the ballast at different test sites can vary and may have a strong influence on the mitigation-measure efficiency. But a measuring procedure to determine the parameters in the track is still not available. Therefore, an indirect procedure is proposed using the field measurement of the track receptance and the laboratory measurements of the resilient-element parameters. Then the ballast stiffness and damping can be obtained by comparing the measured receptance with the results of simulations and adjusting the ballast stiffness to obtain a suitable agreement. For these simulations, models have to be used including also the soil behaviour. Those procedures have to be adapted to the specific cases. Describing this procedure in detail is beyond the scope of this report.

3.5 VEHICLE CHARACTERIZATION

General vehicle influence

The same vehicle generates different levels of ground vibration on different sites. Furthermore different types of vehicles generate different levels of ground vibration on a given site. It is obvious that both the vehicle and the track, sub-grade and soil system is influencing the excitation of vibration and the distinction between the influence of rolling stock and infrastructure can sometimes be tricky. However it is safe to say that without the presence of a vehicle no vibrations are excited and one vehicle can be better than the next. When trying to reduce the vibration levels in the ground one crucial aspect to consider must therefore be the vehicle design.

As described in section 3.1.1 and also the state-of-the-art report RIVAS D5.1 [49] the excitation can be divided into the quasi-static, the dynamic and the parametric excitation. The influencing parameters of the vehicle will be different for the two types of excitation. The quasi-static excitation is influenced by the weight, the speed and the geometric properties (wheel and bogie base) of the vehicle. Higher axle loads give rise to higher amplitude of the excitation while the speed and the geometric properties determine the frequency of the excitation. Each axle load can be seen as a point force, moving with the speed of the vehicle, exciting the track. This will give rise to a broad band excitation. However a fixed point on the track will also be excited by a harmonic load which is caused by the repetitive pass-by of individual equidistant axles.

The dynamic excitation is an interaction effect between vehicle and track. The root cause is the irregularities of the contact surfaces which are present on both the wheel and the rail. The unevenness of the wheel tread should therefore be considered as one vehicle parameter important for ground vibration. Since other vehicle parameters, e.g. the braking system may be influent on the deterioration of the wheel tread, these parameters can also be correlated with the ground vibration emissions related to a specific vehicle design. The frequency of the dynamic excitation is determined by the wavelength of the wheel and track unevenness and the speed of the vehicle. The speed is therefore also an important parameter for the dynamic excitation.

Important vehicle parameters

The response of the vehicle and the track on the excitation described above will determine the characteristics and the level of the vibration which is transmitted into the ground. If the vehicle is highly resilient (seen from the wheel-rail contact) and the track is very stiff most of the vibration energy will be absorbed by the vehicle and little will be injected into the ground. The opposite situation would occur with a soft track. Due to the frequency dependent dynamics of the vehicle and the track the situation will be frequency dependent. Focusing on the vehicle, this means that all the elements of the vehicle design, masses, dampers and springs, that determines the dynamics of the vehicle may be important for the generation of ground vibration. In general however the vehicle parts which are strongly coupled to the track will have most influence, e.g. the un-sprung mass or the primary suspension.

The designs of locomotives, passenger vehicles and freight wagons can differ significantly from each other. The complexity of the vehicle suspension may vary from the most basic freight wagon with only a single level of suspension to the more advanced passenger vehicle

with two levels of vertical suspension, and additional spring and damper components acting in other directions. Apart from the design, both axle load and speed will be important parameters to consider. When discussing ground vibration in general and more specifically vehicle influence it is therefore important to be able to reduce the complex vehicle to a more simple model which only takes into account the parameters important for the vibration generation. According to the studies presented in RIVAS D5.1 [49] the un-sprung mass and the primary suspension stiffness show the clearest influence on the dynamically induced vibration while the overall mass influences the quasi-static excitation. A change in the geometric properties of the vehicle has been shown to shift the frequency of the excitation for a given vehicle speed. As described in the previous section speed, wheel condition and braking system are also important parameter when characterizing the vehicle in the context of ground vibration. The list below contains parameters that should be considered when describing vehicles used in field tests or simulations.

1	Carbody mass
2	Bogie frame mass (primary sprung mass)
3	Wheelset mass (unsprung mass)
4	Distance between bogie centres (bogie base)
5	Distance between axles in one bogie (wheel base)
6	Primary suspension stiffness and damping
7	Secondary suspension stiffness and damping
8	Wheel unevenness (roughness and out-of-roundness, OOR)
9	Braking system
10	Vehicle speed

Table 3: Vehicle parameters important for vehicle characterization in the context of ground vibration

Parameter 1-7 in the list can be taken from the technical vehicle specification while the speed and the wheel roughness and OOR have to be measured. Among the two the vehicle speed is the easiest to measure while the roughness and OOR requires more expensive, and time consuming measurement activities which are described in section 3.2.2 of this document.

Modelling vehicle receptance A_W

In the simulation studies in the RIVAS project the vehicle is represented by its vehicle receptances. These are calculated by using multi-body models of the vehicle which contain information about parameter 1-7 listed above. The vehicle receptance describes the wheel displacements resulting from an applied force in the wheel-rail contact, both for the excitation and response at the same wheel (point receptance) and for excitation at one wheel and response at another wheel (cross receptance). The vehicle receptances could also be measured by elevating the vehicle, mounting displacement sensors on each wheel and exciting one wheel at a time by e.g. an impact hammer or a shaker. The methods described in

the RIVAS project will however only consider calculated receptances due to the high costs associated with measurement campaigns.

There are different tools for calculating the receptances of a vehicle and a good overview of available tools is given in RIVAS D5.1 [49]. Figure 17 illustrates a basic model which is used to calculate the vertical vehicle receptances including the pitch motion of the carbody and bogie frame (rotation about the y-axis). The TRAFFIC software developed by K.U Leuven which is used for predicting the far field ground vibration within RIVAS include a basic model similar to this which considers parameter 1-7 in the list above.

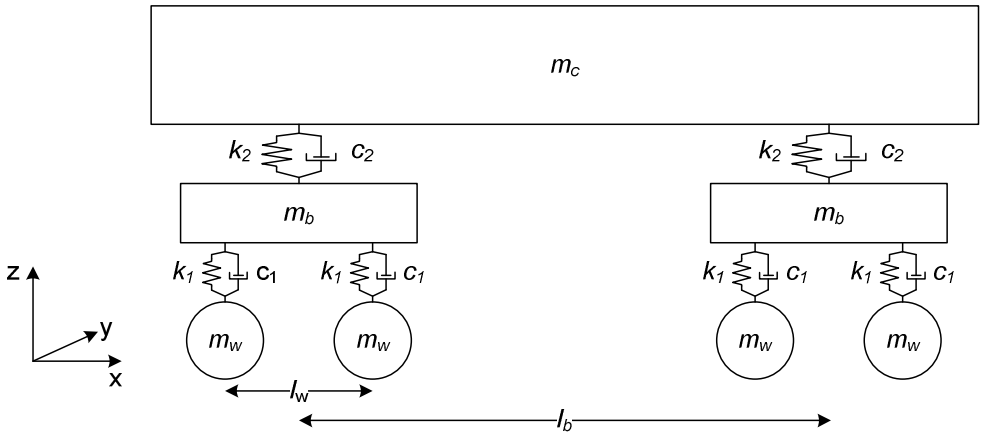

Figure 17: Vehicle model for calculation of vehicle receptances. Vertical motion and rotation about the y-axis are considered.

An alternative model which can include a more complex vehicle design is the multi-body model used by the vehicle manufacturer for prediction of the vehicle dynamics and ride stability. There are several different tools for these calculations e.g. SIMPACK, ADAMS and GENSYS which are described in RIVAS D5.2. Figure 18 shows an example of vehicle receptances calculated from a model like the one in figure 17. Both point and cross receptances are included.

As expected the point receptance in figure 18 is generally higher than the cross-receptances. Around 2 Hz the secondary suspension resonance is seen while the resonance of the primary suspension around 8 Hz is strongly damped. The inertia of the un-sprung mass leads to a high dynamic stiffness of the vehicle at higher frequencies which is seen in the sloping receptance above the resonance frequency of the primary suspension.

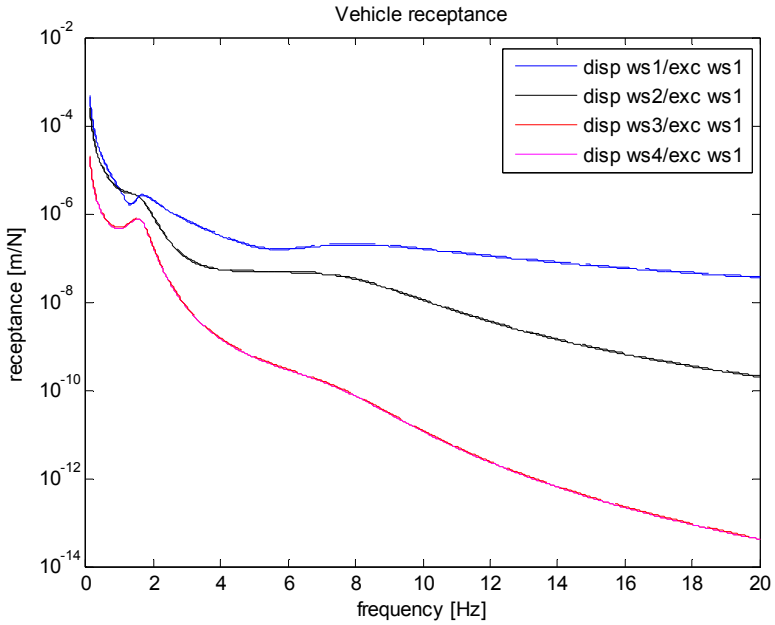

Figure 18: Vehicle receptances calculated with a basic vehicle model as described by figure 17

3.6 SUMMARY AND CONCLUSION

The aim of the deliverable D 1.2 Annex is to provide measurement protocols for parameters influencing the mitigation-measure efficiency.

In section 3.1, a simplified modelling approach based on the rail unevenness U_R, the wheel unevenness U_W, the track receptance A_R, the vehicle receptance U_W, and the transfer function H was presented. For the measurement, there are two possibilities to characterize the measuring and the reference conditions. First, the influencing parameters U_R, U_W, A_R, A_W and H can be measured directly. The second possibility includes calculation of U_R, U_W, A_R, A_W and H based on measurements of the basic parameters (e. g. by knowing the masses and the elastic properties of the vehicle suspension, the vehicle receptance A_W can be calculated by using simple models). Both approaches were considered in this report.

In section 3.2, methods to detect wheel and rail unevenness (U_R, U_W) as well as the stiffness variation along the track were described. Section 3.3 summarizes the measurement protocol to determine dynamic soil characteristics and transfer functions H. For the track characterization, a measuring protocol for the track receptance A_R as well as for the stiffness and damping of resilient elements in the track can be found in section 3.4. As discussed in section 3.5, the vehicle receptance A_W is typically calculated by using the stiffness and damping of the primary suspension and the masses included.

The measuring protocols for the different influencing parameters differ in the degree of detail. Where ever possible, reference is made to standards and the description is kept brief. But if no standards are available, as for the soil characterization or the measurement of the wheel unevenness the measuring protocols are more detailed. Although the authors are aware that e. g. the measurement protocol for the ballast parameters is missing, it was decided to make the document accessible to the partners as soon as possible. If new results are obtained within the RIVAS project, the document can be updated if necessary.

4. REFERENCES

[1] Project RIVAS, Description of Work, 2010

[2] Project RIVAS, Del 1.2, Protocol for free field measurements of mitigation effects in the project RIVAS for WP 2, 3, 4, 5, October 2011

[3] G. Lombaert, G. Degrande, J. Kogut, and S. François, The experimental validation of a numerical model for the prediction of railway induced vibrations, Journal of Sound and Vibration, vol. 297(3-5), 512-535, 2006

[4] EN 15610, Railway applications – Noise emission – Rail roughness measurement related to rolling noise generation, EN 15610:2009

[5] P. Fodiman, NOEMIE Project Final report (Project 2002/EU/1663), AEIF, July 2005, see Appendix D

[6] EN ISO 266, Acoustics – Preferred frequencies, ISO 266:1997

[7] N. Triepaischajonsak, D.J. Thompson, C.J.C. Jones, J. Ryue and J.A. Priest, Ground vibration from trains: experimental parameter characterisation and validation of a numerical model. Proceedings of the Institution of Mechanical Engineers, Part F: Journal of Rail and Rapid Transit 225, 140-153, 2011

[8] Eric Berggren, PhD Thesis, *Railway Track Stiffness, Dynamic Measurements and Evaluation for Efficient Maintenance*, 2009

[9] S. Iwnicki and T. Dahlberg, "Handbook of Railway Vehicle Dynamics," *System*, pp. 143-179, 2006

[10] Project RIVAS, Deliverable D 1.1, Test procedures for the determination of the dynamic soil characteristics, December 2011

[11] S. Nazarian and M.R. Desai, Automated surface wave method: field testing. Journal of Geotechnical Engineering, Proceedings of the ASCE, 119(7):1094–1111, 1993

[12] D. Yuan and S. Nazarian, Automated surface wave method: inversion technique. Journal of Geotechnical Engineering, Proceedings of the ASCE, 119(7):1112–1126, 1993

[13] S. Nazarian and K.H. Stokoe II, Nondestructive testing of pavements using surface waves, Transportation Research Record, 993:67–79, 1984

[14] V. Cuellar and J. Valerio, Use of the SASW method to evaluate soil improvement techniques. In Proceedings of the 14th International Conference Soil Mechanics and Foundation Engineering, pages 461–464, Hamburg, 1997

[15] E. Kavazanjian, M.S. Snow, C.J. Poran, and T. Satoh, Non-intrusive Rayleigh wave investigations at solid waste landfills, In Proceedings of the First International Congress on Environmental Geotechnics, pages 707–712, Edmonton, 1994

[16] H.R. Masoumi, G. Degrande, and G. Lombaert, Prediction of free field vibrations due to pile driving using a dynamic soil-structure interaction formulation, Soil Dynamics and Earthquake Engineering, 27(2):126–143, 2007

[17] L. Pyl, G. Degrande, G. Lombaert, andW. Haegeman, Validation of a source-receivermodel for road traffic induced vibrations in buildings. I: Source model, ASCE Journal of Engineering Mechanics, 130(12):1377–1393, 2004

[18] C.G. Lai, Simultaneous inversion of Rayleigh phase velocity and attenuation for near-surface site characterization, PhD thesis, Georgia Institute of Technology, 1998

[19] G.J. Rix, C.G. Lai, and A.W. Spang Jr., In situ measurement of damping ratio using surface waves. Journal of Geotechnical and Geoenvironmental Engineering, Proceedings of the ASCE, 126(5):472–480, 2000

[20] C.G. Lai, G.J. Rix, S. Foti, and V. Roma, Simultaneous measurement and inversion of surface wave dispersion and attenuation curves, Soil Dynamics and Earthquake Engineering, 22(9-12):923–930, 2002

[21] J. Xia, R.D. Miller, C.B. Park, and G. Tian, Determining Q of near-surface materials from Rayleigh waves, Journal of Applied Geophysics, 51(2-4):121–129, 2002

[22] S. Foti, Using transfer function for estimating dissipative properties of soils from surfacewave data, Near Surface Geophysics, 2:231–240, 2004

[23] M. Schevenels, S.A. Badsar, and G. Degrande, Application of the SASW method for the determination of stiffness and damping parameters of soils, International Seminar on Interaction Soil-Railway-Track for High Speed Railways, Geotechnical aspects. LNEC, Lisbon, Portugal. Invited lecture, September 2008

[24] C.B. Park, R.D. Miller, and J. Xia, Imaging dispersion curves of surface waves on multichannel record, In Proceedings of the 68th Annual International Meeting, Society of Exploration Geophysicists, Expanded abstracts, pages 1377–1380, New Orleans, Louisiana, U.S.A., 1998

[25] C.B. Park, R.D. Miller, and J. Xia, Multichannel analysis of surface waves, Geophysics, 64(3):800–808, 1999

[26] D.J. Ewins, Modal testing: theory and practice. Research Studies Press Ltd., Letchworth,UK, 1984

[27] M. Schevenels, The impact of uncertain dynamic soil characteristics on the prediction of ground vibrations, PhD thesis, Department of Civil Engineering, KU Leuven, 2007

[28] S.A. Badsar, M. Schevenels, and G. Degrande, Determination of the dynamic soil properties with the SASW method on the Arenberg III campus in Heverlee. Technical Report BWM-2009-05, Department of Civil Engineering, KU Leuven, March 2009

[29] C.B. Park, R.D. Miller, N. Ryden, J. Xia, and J. Ivanov, Combined use of active and passive surface waves. Journal of Environmental and Engineering Geophysics, 10(3):323–334, 2005

[30] S.A. Badsar, M. Schevenels, W. Haegeman, and G. Degrande. Determination of the damping ratio in the soil from SASW tests using the half-power bandwidth method. Geophysical Journal International, 182(3):1493–1508, 2010

[31] S.A. Badsar, In situ determination of material damping in the soil at small deformation ratios, PhD thesis, Department of Civil Engineering, KU Leuven, 2012.

[32] E. Kausel and J.M. Roësset, Stiffness matrices for layered soils, Bulletin of the Seismological Society of America, 71(6):1743–1761, 1981

[33] M. Schevenels, S. François, and G. Degrande, EDT: An ElastoDynamics Toolbox for MATLAB, Computers & Geosciences, 35(8):1752–1754, 2009

[34] N. Gucunski and R.D. Woods, Inversion of Rayleigh wave dispersion curve for SASW test. In Proceedings of the 5th International Conference on Soil Dynamics and Earthquake Engineering, pages 127–138, Karlsruhe, 1991

[35] K. Tokimatsu, S. Tamura, and H. Kosjima, Effects of multiple modes on Rayleigh wave dispersion characteristics. Journal of Geotechnical Engineering, Proceedings of the ASCE, 118(10):1529–1143, 1992

[36] M. Schevenels, G. Lombaert, G. Degrande, and S. François, A probabilistic assessment of resolution in the SASW test and its impact on the prediction of ground vibrations, Geophysical Journal International, 172(1):262–275, 2008

[37] M. Schevenels, G. Lombaert, G. Degrande, and M. Arnst, Measurement and prediction of the soil's transfer function at a site in Lincent. Technical Report BWM-2006-03, Department of Civil Engineering, KU Leuven, February 2006

[38] M. Schevenels, G. Lombaert, and G. Degrande, Determination of the dynamic soil properties by refracted P-wave and surface wave characterization at a site in Lincent (Belgium), report BWM-2011-17, Department of Civil Engineering, KU Leuven, September 2011

[39] M.Withers, R. Aster, C. Young, J. Beiriger, M. Harris, S. Moore, and J. Trujillo, A comparison of select trigger algorithms for automated global seismic phase and event detection, Bulletin of the Seismological Society of America, 88(1):95–106, 1998

[40] The MathWorks, MATLAB Optimization Toolbox User's Guide, 2011

[41] B. Cauberghe, Applied frequency-domain system identification in the field of experimental and operational modal analysis, PhD thesis, Vrije Universiteit Brussel, 2004

[42] S.O. Rice, Mathematical analysis of random noise, Bell System Technical Journal, 24:45–156, 1945

[43] H. Verbraken, P. Coulier, G. Lombaert, and G. Degrande, Measurement of train passages and transfer functions at a site in Lincent, Report BWM-2012-05, Department of Civil Engineering, KU Leuven, May 2012

[44] H. Verbraken, G. Lombaert, and G. Degrande, Benchmark tests for soil properties, including recommendations for standards and guidelines, RIVAS project SCP0-GA-2010-265754, Deliverable D1.11, Report to the EC, December 2013, draft version

[45] DIN 45673 Mechanical vibration - Resilient elements used in railway tracks
- Part 1: Terms and definitions, classification, test procedures, 2010
- Part 2: Determination of static and dynamic characteristics in the track under operation, 2008
- Part 3: Experimental evaluation of insertion loss from artificial excitation of mounted track systems (in a test rig and in situ), prenorm 2004
- Part 4: Analytical evaluation of insertion loss of mounted track systems, 2008
- Part 5: Laboratory test procedures for under-ballast mats, 2010
- Part 6: Laboratory test procedures for under-sleeper pads of concrete sleepers, 2010

- Part 7: Laboratory test procedures for resilient elements of floating slab track systems, 2011
- Part 8: Laboratory test procedures for continuous elastic rail supports, 2010
- Part 9: Laboratory test procedures for resilient elements of rail fastening systems and for discrete rail supports[1]

[46] EN ISO 10846 "Acoustics and vibration – Laboratory measurement of vibro-acoustic transfer properties of resilient elements":

- Part 1: Principles and guidelines, 2011
- Part 2: Dynamic stiffness of elastic supports for translatory motion – Direct method, 2011

[47] EN 13146-9 (E) Railway applications - Track - Test methods for fastening systems – Part 9: Determination of stiffness, 2011.

[48] ENV 13481-6 Railway applications - Track - Performance requirements for fastening systems: Part 6: Special fastening systems for attenuation of vibration, 2002

[49] Project RIVAS, Del. 5.1, Train Induced Ground Vibration – Influence of Rolling Stock, State-of-the-Art Survey, September 2012

[1] Currently under preparation as a supplement to DIN EN 13146-9 which already contains a number of specifications on the determination of stiffness in rail fastening systems.